Phospholipid flippases Lem3p-Dnf1p and Lem3p-Dnf2p are involved in the sorting of the tryptophan permease Tat2p in yeast*

Takeru Hachiro, Takaharu Yamamoto, Kenji Nakano, and Kazuma Tanaka[1]

From the Division of Molecular Interaction, Institute for Genetic Medicine, Hokkaido University Graduate School of Life Science, N15 W7, Kita-ku, Sapporo, 060-0815, Japan

*Running title: *Phospholipid asymmetry is involved in localization of Tat2p*

[1]To whom correspondence should be addressed: Kazuma Tanaka, Division of Molecular Interaction, Institute for Genetic Medicine, Hokkaido University Graduate School of Life Science, N15 W7, Kita-ku, Sapporo, 060-0815, Japan. Tel.: +81–11–706–5165; Fax: +81–11–706–7821; E-mail: k-tanaka@igm.hokudai.ac.jp.

Keywords: phospholipid asymmetry; type 4 P-type ATPase; flippase; tryptophan permease; ubiquitination; yeast

---

Background: Lem3p-Dnf1p and -Dnf2p are phospholipid flippases that generate phospholipid asymmetry in yeast.
Results: The tryptophan permease Tat2p is missorted from the *trans*-Golgi network to the vacuole in the *lem3*Δ mutant.
Conclusion: Phospholipid asymmetry supports plasma membrane transport of Tat2p by inhibiting its improper ubiquitination at the *trans*-Golgi network.
Significance: Phospholipid asymmetry may be involved in proper sorting of membrane proteins.

SUMMARY

The type 4 P-type ATPases are flippases that generate phospholipid asymmetry in membranes. In budding yeast, heteromeric flippases including Lem3p-Dnf1p and -Dnf2p translocate phospholipids to the cytoplasmic leaflet of membranes. Here we report that Lem3p-Dnf1/2p are involved in transport of the tryptophan permease Tat2p to the plasma membrane. The *lem3*Δ mutant exhibited tryptophan requirement due to the mislocalization of Tat2p to intracellular membranes. Tat2p was relocalized to the plasma membrane when *trans*-Golgi network (TGN)-to-endosome transport was inhibited.

Inhibition of ubiquitination by mutations in ubiquitination machinery also rerouted Tat2p to the plasma membrane. Lem3p-Dnf1/2p are localized to endosomal/TGN membranes in addition to the plasma membrane. Endocytosis mutants, in which Lem3p-Dnf1/2p are sequestered to the plasma membrane, also exhibited the ubiquitination-dependent missorting of Tat2p. These results suggest that Tat2p is ubiquitinated at the TGN and missorted to the vacuolar pathway in the *lem3*Δ mutant. The NH_2-terminal cytoplasmic region of Tat2p containing ubiquitination acceptor lysines interacted with liposomes containing acidic phospholipids including phosphatidylserine. This interaction was abrogated by alanine substitution mutations in the basic amino acids downstream of the ubiquitination sites. Interestingly, a mutant Tat2p containing these substitutions was missorted in a ubiquitination-dependent manner. We propose the following model based on these results: Tat2p is not ubiquitinated when the NH_2-terminal region is bound to membrane phospholipids, but if it dissociates from the membrane due to a low level of phosphatidylserine caused by perturbation of phospholipid asymmetry in the *lem3*Δ mutant, Tat2p is ubiquitinated and then transported from the TGN to the vacuole.

INTRODUCTION

Phospholipid asymmetry of bilayer membranes is generally observed in the plasma membrane of eukaryotic organisms. In this phospholipid asymmetry, phosphatidylcholine $(PC)^2$ is predominantly distributed in the outer leaflet facing extracellular space (exoplasmic leaflet), whereas phosphatidylethanolamine (PE) and phosphatidylserine (PS) are distributed in the inner leaflet facing cytoplasm (cytoplasmic leaflet). The type 4 subfamily of P-type ATPase (P4-ATPase) seems to play an essential role to generate, maintain, and regulate phospholipid asymmetry by working as a "flippase", which translocates aminophospholipids from the exoplasmic leaflet to the cytoplasmic one in an energy-dependent manner (1-5).

Five P4-ATPases, i.e., Drs2p, Dnf1p, Dnf2p, Dnf3p, and Neo1p are identified in the budding yeast *Saccharomyces cerevisiae* and these proteins except Neo1p require Cdc50-family proteins as non-catalytic subunits for their localization, function, and flippase activity (6-10). Drs2p, Dnf1p and Dnf2p, and Dnf3p are complexed with Cdc50p, Lem3p, and Crf1p, respectively. Drs2p is localized to endosomes, the *trans*-Golgi network (TGN), and post-Golgi secretory vesicles (11-13), whereas Dnf1p and Dnf2p are localized to the plasma membrane and early endosome/TGN membranes (13-15). Dnf1p and Dnf2p seem to be directly regulated by two serine/threonine kinases Fpk1p and Fpk2p (15). Functional studies revealed that flippases are involved in various vesicle transport pathways (5), and flippases in these functions are implicated in vesicle formation by inducing local membrane curvature (16,17). Flippases also regulate functions of membrane proteins by changing transbilayer phospholipid

composition: changes in PE and PS content in the cytoplasmic leaflet of the plasma membrane regulate Cdc42p localization in polarized cell growth (18,19). However, other functions of flippases need to be investigated.

Tat2p is a high-affinity tryptophan permease, which is the main machinery for tryptophan uptake in budding yeast. Similar to other permeases, localization of this permease is precisely regulated responding to extracellular tryptophan concentration: at low tryptophan, Tat2p is transported to the plasma membrane, but it is transported from the TGN to the vacuole at high tryptophan (20). Localization of yeast permeases is regulated by ubiquitination. Especially, monoubiquitination and lysine 63-linked polyubiquitin chain direct target permeases to the vacuole from the plasma membrane or from the sorting compartment without going through the plasma membrane (21). In the case of Tat2p, five lysine residues in the NH_2-terminal cytoplasmic domain are identified as ubiquitin acceptor sites, which are recognized by ubiquitin ligase complexes Rsp5p-Bul1p and -Bul2p (20,22).

Several reports have shown that changes in membrane lipid environment cause tryptophan requirement, probably due to mislocalization of Tat2p to the vacuole. Tat2p was inappropriately ubiquitinated in the *erg6*Δ mutant, which has a defect in the last step of ergosterol biosynthesis, and resulted in the missorting of Tat2p to the vacuole (20). The *cho1*Δ mutant, which is defective in phosphatidylserine synthesis, exhibited impaired tryptophan uptake (23). Fluidization of membrane lipids by increased unsaturation of fatty acids also caused tryptophan requirement (24). However, little is known about how Tat2p is missorted to the vacuole by changes in lipid microenvironment.

Here we show that Tat2p is also missorted to the vacuole by ubiquitination at the TGN in the *lem3*Δ mutant. Our results suggest that the destination of Tat2p is regulated by the interaction of its NH_2-terminal region with phospholipids including phosphatidylserine in the cytoplasmic leaflet of membranes.

EXPERIMENTAL PROCEDURES

Media and genetic methods-Cells were cultivated in YP-based rich medium (1% Bacto-yeast extract [Difco Laboratories, Detroit, MI], 2% Bacto-peptone [Difco], 2% glucose, and 0.01% adenine) supplemented with (YPDAW) or without (YPDA) 200 μg/ml tryptophan. Strains carrying plasmids were selected in synthetic medium (SD) containing the required nutritional supplements (25). Synthetic complete medium (SC) was SD medium containing all required nutritional supplements. When indicated, 0.5% casamino acids were added to SD medium with (SDA) or without (SDA-U) 20 μg/ml uracil. Tryptophan was supplemented to SDA medium at a concentration of 200 μg/ml (SDA200W) or 30 μg/ml (SDA30W), or was not supplemented (SDA-W). Standard genetic manipulations of yeast were performed as described previously (26).

Escherichia coli strains DH5α and XL1-Blue were used for construction and amplification of plasmids. The lithium acetate method was used for introduction of plasmids into yeast cells (27,28).

Strains and plasmids-Yeast strains used in this study are listed in **Table 1**. The *vps27*Δ and *TAT2-3HA* strains were constructed by transforming a BY4743 background strain (29) with the 3.6-kb *Eco*RI-*Sal*I fragment from pKU65 and *Pma*CI-digested pKU51 (gifts from A. Nakano, Riken, Saitama, Japan), respectively. Other strains carrying complete gene deletions, GFP-tagged *DNF1* and *DNF2*, and monomeric red fluorescence protein 1 (mRFP)-tagged *SEC7* were constructed in the BY4743 background by PCR-based procedures as described (30,31). All strains constructed by the PCR-based procedure were verified by colony-PCR amplification to confirm that the replacement had occurred at the expected locus. To construct the $TAT2^{3K>R}$ mutant, *tat2*Δ*::KanMX4* was transformed with the 2.9-kb *Pst*I-*Eco*RI fragment of $TAT2^{3K>R}$ from pKT2008, and the transformants were screened for tryptophan prototrophy on a YPDA plate. The transformant which lost the *KanMX4* marker was further selected. The *rsp5-1* mutant was constructed by two successive backcrosses to a BY4743 background strain.

The plasmids used in this study are listed in **Table 2**. Schemes detailing the construction of plasmids and DNA sequences of nucleotide primers are available on request. Site-directed mutations were introduced into the NH_2-terminal region of Tat2p by the overlap extension PCR method using pKT1747 as a template (32). The PCR-amplified region in each construct was sequenced to verify that only the desired mutations were introduced.

Sucrose gradient fractionation-Fractionation of subcellular organelles based on sedimentation through a sucrose step gradient was performed as described previously (33) with a slight modification. In brief, 50 OD_{600} units of early log phase cells were harvested and washed with ice-cold 10 mM NaN_3. The cells were collected by centrifugation and resuspended in 0.5 ml STE10 buffer [10% sucrose (w/w), 10 mM Tris-HCl, pH7.5, and 10 mM EDTA] with protease inhibitors (1 μg/ml aprotinin, 1 μg/ml leupeptin, and 1 mM PMSF), followed by agitation with glass beads. After addition of 1 ml STE10 buffer with protease inhibitors, unlysed cells and debris were removed by centrifugation (500 × g for 3 min). 0.2 ml of the total cell lysate was subjected to centrifugation on a three-step sucrose gradient [0.2 ml of 55%, 0.5 ml of 45%, and 0.4ml of 30% sucrose (w/w) in 10 mM Tris-HCl, pH 7.5, and 10 mM EDTA] at 55,000 rpm in a TLS55 rotor (Beckman, Brea, CA) for 2.5 h. Fractions (0.2 ml) were collected manually from the top and analyzed by immunoblotting, which was performed as described previously (34). For membrane proteins, SDS-PAGE samples were heated at 37°C for 30 min before loading. Protein bands were visualized by chemiluminescence using ECL or ECL advance (GE Healthcare, Little Chalfont, Buckinghamshire,

England). Where indicated, only the results of plasma membrane-rich fractions are shown.

Microscopy-GFP-tagged Dnf1p and Dnf2p were observed in living cells, which were grown to early log phase, collected, and resuspended in SC medium. Cells were mounted on microslide glass and immediately observed. Co-localization of Dnf1p-GFP or Dnf2p-GFP with Sec7-mRFP was examined in fixed cells. Fixation was performed by addition of a commercial 37% formaldehyde stock (Wako Pure Chemicals, Osaka, Japan) to a final concentration of 3.7% in the medium, followed by a 10-min incubation at 30°C. After fixation, cells were washed twice with phosphate-buffered saline and examined.

Cells were observed using a Nikon ECLIPSE E800 microscope (Nikon Instec, Tokyo, Japan) equipped with an HB-10103AF super high pressure mercury lamp and a 1.4 NA 100× plan Apo oil immersion objective with the appropriate fluorescence filter sets and differential interference contrast optics. Images were acquired with a digital cooled charge-coupled device camera (C4742-95-12NR; Hamamatsu Photonics, Hamamatsu, Japan) using AQUACOSMOS software (Hamamatsu Photonics). Observations are compiled from the examination of at least 200 cells.

Liposome flotation experiments-Binding of the Tat2p NH_2-terminal fragment to liposomes was assayed by liposome flotation experiments (35). The NH_2-terminal cytoplasmic region (residues 1-85) of Tat2p (Tat2pNT) and its mutant proteins were expressed and purified as a GST fusion protein from the cells of yeast KKT452 (*pep4*Δ *prb1*Δ *TRP1*) containing pKT2026, pKT2027, pKT2028, or pKT2029 as described (15) with the following modifications. In ammonium sulfate precipitation, the fraction that precipitated between 15 and 35% (wt/vol) salt saturation was used. In affinity purification with Glutathione Sepharose 4B (GE Healthcare), the column was washed three-times with 3.3 bed volumes of 20 mM HEPES buffer (pH8.0) after loading the sample, and GST fusion proteins were successively eluted five times with one bed volume of the same buffer containing 10 mM reduced glutathione. Liposomes were prepared as follows. A dried film, prepared by evaporation of a mixture of defined lipids in chloroform, was resuspended in 20 mM HEPES buffer (pH7.2), followed by brief sonication. After five steps of freezing and thawing in liquid nitrogen, the liposome suspension was extruded through a polycarbonate filter (pore size 0.1 μm, GE Healthcare) using LiposoFast (Avestin, Ottawa, Canada). Liposomes were stored at room temperature and used within 2 days after preparation. Lipids used were dioleoylphosphatidylcholine (DOPC), dioleoylphosphatidylethanolamine (DOPE), dioleoylphosphatidylserine (DOPS), and L-α-phosphatidic acid (PA) (Avanti Polar Lipids, Alabaster, AL) and L-α-phosphatidylinositol (PI) (Nacalai Tesque, Kyoto, Japan). A fluorescence [7-nitrobenz-2-oxa-1,3-diazol-4-yl (NBD)]–

labeled PE, 1-palmitoyl-2-(6-NBD-aminocaproyl)-PE (Avanti Polar Lipids), was added to every liposomes at 0.2 mol% to visualize flotation of liposomes. Liposome flotation assay was modified as follows. GST-Tat2pNT or its mutant protein (1 μM) was incubated at 30°C for 5 min with liposomes (1 mM lipids) in 20 mM HEPES buffer (pH7.2). The suspension was then adjusted to 30% (wt/vol) sucrose and sequentially overlaid with 25% and 0% sucrose in 20 mM HEPES buffer (pH7.2), followed by centrifugation at 20°C for 1 h. The top (0.1 ml), middle (0.2 ml), and bottom (0.25 ml) fractions were manually collected, and proteins were precipitated with 10% TCA. After washing twice with 1 ml of cold acetone, the pellet was air dried and resuspended in SDS-PAGE sample buffer. After SDS-PAGE, proteins were stained with SYPRO RED (Lonza, Rockland, ME), followed by quantification with a FLA-3000 fluorescence imaging system (Fuji Photo Film, Tokyo, Japan).

Tryptophan uptake assay-Tryptophan uptake was assayed as follows based on a previous study (36). Cells were grown to early log phase in SDA-W medium at 30°C. 0.9 OD_{600} units of the cells were washed twice with wash buffer [10 mM sodium citrate, pH4.5, and 20 mM $(NH_4)_2SO_4$]. The cells were then resuspended in 2.7 ml of incubation medium [10 mM sodium citrate, pH4.5, 20 mM $(NH_4)_2SO_4$, and 2% glucose], and the optical density at 600 nm was measured. The assay was initiated by the addition of 300 μl of radiolabeled tryptophan solution (297 μl of the incubation medium and 3 μl of L-[5-^{3}H]tryptophan, 20 Ci/mmol; American radiolabeled Chemicals, St. Louis, MO) at a final tryptophan concentration of ~ 10 μg/ml. An aliquot (500 μl) was withdrawn at each time point and chilled by the addition of 1 ml of the ice-cold incubation medium. The cells were collected by filtration through a nitrocellulose filter (pore size 0.45 μm, Schleicher Schuell Bioscience, Dassel, Germany) presoaked in the wash buffer and washed three times with chilled water. The filters were completely dried at 50°C for more than 2 h, and intracellular radiolabeled tryptophan was quantified by scintillation counting.

When tryptophan import activity of Tat2p was estimated (Fig. 7*B*), the Tat2p content in the plasma membrane was determined. Cells were grown to early log phase in SDA-UW medium at 30°C. 50 OD_{600} units of the cells were subjected to the sucrose gradient fractionation as described above to obtain the plasma membrane-rich fraction, which was analyzed by immunoblotting. The Tat2p content was quantified by densitometric scanning with LAS-1000 (Fuji Photo Film). Other 3.5 OD_{600} units of the cells instead of 0.9 OD_{600} units were subjected to tryptophan uptake assay as described above. The data (10^4 dpm/OD_{600}) were corrected for the difference of Tat2p content in the plasma membrane-rich fraction.

Antibodies-Rabbit anti-Tat2p polyclonal antibodies were generated against two synthetic peptides of 17 amino acids, N1 (residues 5-21) and

N2 (residues 66-82), from the NH_2-terminal cytoplasmic tail of Tat2p. Peptide synthesis and rabbit immunizations were performed in MBL (Nagoya, Japan). Antibodies were affinity-purified with a protein column in which 5 mg of GST-Tat2pNT (residues 1-85) was coupled to 0.5 ml of CNBr-activated Sepharose 4B beads (GE Healthcare). GST-Tat2pNT was expressed in *E. coli* and purified as described previously (37). The antiserum was incubated with the protein beads for 1 h at room temperature with gentle rotation. The beads were then successively washed five times with 1 ml of high salt wash buffer (50 mM Tris-HCl, pH7.5, and 500 mM NaCl) and five times with 1 ml of low salt wash buffer (50 mM Tris-HCl, pH7.5, and 150 mM NaCl). The antibodies were successively eluted five times with 0.5 ml of 0.1 M glycine-HCl (pH3.5) and five times with 0.5 ml of 0.1 M glycine-HCl (pH2.5), and the eluates were immediately equilibrated to pH7.5 by mixing with 1 M Tris-HCl (pH8.5). Fractions were divided into aliquots and stored at -20°C. The antibodies against the N1 and N2 peptides were named anti-Tat2pN1 and anti-Tat2pN2 antibodies, respectively. Mouse anti-Pep12p monoclonal antibody was purchased from Life Technologies (Carlsbad, CA). Rabbit anti-Kex2p and -Pma1p polyclonal antibodies were gifts from S. Nothwehr (University of Missouri, Columbia, MO) and R. Serrano (Polytechnic University of Valencia, Valencia, Spain), respectively. For immunoblot analyses, these antibodies were used at the following dilution: anti-Pep12p, 1:1000; anti-Kex2p, 1:5000; anti-Pma1p, 1:50,000; anti-Tat2pN1, 1:10,000; anti-Tat2pN2, 1:5000. Horseradish peroxidase (HRP)-conjugated secondary antibodies (sheep anti-mouse IgG and donkey anti-rabbit IgG) used for immunoblotting were purchased from GE Healthcare.

RESULTS

The flippase mutants are defective in tryptophan uptake because of dysregulation of Tat2p-The *TRP1* gene product (phosphoribosylanthranilate isomerase) catalyzes the third step in the tryptophan biosynthesis pathway in budding yeast (38). Thus, *trp1*Δ cells require extracellular tryptophan for growth. As shown in **Fig. 1*A***, *trp1*Δ cells grew normally in YPDA rich medium containing tryptophan at a standard concentration (~ 100 μg/ml), which was estimated by amino acid compositional analysis (our unpublished results). Tryptophan uptake at this tryptophan concentration is thought to mainly depend on a high-affinity tryptophan permease, Tat2p (39). Thus, *tat2*Δ *trp1*Δ cells did not grow on YPDA, but grew on YPDAW, which contained a high concentration of tryptophan (~ 300 μg/ml), since tryptophan could be taken up by a low-affinity tryptophan permease, Tat1p (39) (**Fig. 1*A***). We previously identified Fpk1p and Fpk2p as kinases that phosphorylated Dnf1p and Dnf2p flippases for activation (15). We noticed that *fpk1*Δ *fpk2*Δ *trp1*Δ cells did not grow on YPDA, but on YPDAW (**Fig. 1*A***). Consistently, *dnf1*Δ *dnf2*Δ

*trp1*Δ as well as *lem3*Δ *trp1*Δ cells also exhibited tryptophan requirement, albeit weakly (**Fig. 1*A***). Similar tryptophan requirement was also observed in *drs2*Δ *trp1*Δ and *cdc50*Δ *trp1*Δ mutants, but the phenotype seems to be milder compared to the *dnf1*Δ *dnf2*Δ/*lem3*Δ *trp1*Δ mutants, because the *drs2*Δ/*cdc50*Δ *trp1*Δ mutants exhibited slower growth even in YPDAW medium. Tryptophan requirement was not seen in the *dnf3*Δ/*crf1*Δ *trp1*Δ mutants (our unpublished results). These results suggest that the tryptophan requirement of *lem3*Δ and *dnf1*Δ *dnf2*Δ mutants reflects a unique function of Lem3p-Dnf1/2p. The severest tryptophan requirement in the *fpk1*Δ *fpk2*Δ *trp1*Δ mutant could be due to reduced phosphorylation of Drs2p, Ypk1p, or other substrates in addition to Dnf1p/Dnf2p (15,40). The *dnf1*Δ *dnf2*Δ *trp1*Δ and *lem3*Δ *trp1*Δ mutants exhibited clearer tryptophan-dependent growth at 18°C (**Fig. 1*B***). Interestingly, the *tat2*Δ *trp1*Δ mutant did not grow even in YPDAW, suggesting that the function or localization of Tat1p may be impaired at 18°C. The *cho1*Δ *trp1*Δ mutant also exhibited tryptophan requirement for growth as reported previously (23), but it grew slowly even in YPDAW (**Fig. 1*A***).

These results suggest that the tryptophan requirement in the *dnf1*Δ *dnf2*Δ/*lem3*Δ *trp1*Δ mutant is caused by dysregulation of Tat2p, and this was supported by the following results. (i) The tryptophan requirement of *lem3*Δ *trp1*Δ, *fpk1*Δ *fpk2*Δ *trp1*Δ, and *cho1*Δ *trp1*Δ mutants was suppressed by the overexpression of *TAT2* (**Fig. 1*C***). (ii) The *tat2*Δ mutation is synthetically lethal with the *tat1*Δ mutation in the *trp1*Δ background due to the severe uptake defect of tryptophan (39). The *lem3*Δ *trp1*Δ mutation was synthetically lethal with *tat1*Δ, but not with *tat2*Δ (**Fig. 1*D***). Our strain background contains not only *trp1*Δ but also *leu2*Δ, *his3*Δ, *met15*Δ and *lys2*Δ mutations, but the *lem3*Δ mutant did not require a higher level of these amino acids for growth (our unpublished results), suggesting that dysregulation of an amino acid transporter is specific to Tat2p.

The plasma membrane Tat2p is decreased in the lem3Δ mutant-Our previous microarray analysis suggested that the *lem3*Δ mutation did not affect transcription of *TAT2* (our unpublished results). To investigate intracellular localization of Tat2p, we constructed tagged versions of Tat2p, in which GFP, GST, thirteen copies of the myc epitope (13myc), and three copies of the HA epitope (3HA) were appended at the COOH-terminus of *TAT2* in the genomic locus. However, *TAT2-GFP*, *TAT2-GST*, and *TAT2-13myc* resulted in suppression of the tryptophan requirement in the *lem3*Δ *trp1*Δ mutant, whereas *TAT2-3HA* was non-functional in the *tat2*Δ mutant (**Fig. 2*A*** and ***B***). *TAT2-GFP* also suppressed the tryptophan requirement in the *fpk1*Δ *fpk2*Δ *trp1*Δ and *cho1*Δ *trp1*Δ mutants (our unpublished results). We also constructed the NH_2-terminally tagged versions of Tat2p, but again they did not complement the *tat2*Δ mutation (**Fig. 2*C***). Therefore, we decided to generate antibodies against Tat2p.

Anti-Tat2p polyclonal antibodies were

generated in rabbits against two Tat2p peptides (N1, residues 5-21, and N2, residues 66-82) from the NH_2-terminal cytoplasmic region of Tat2p. As shown in **Fig. 3*A***, Tat2p was detected as a band of about 50 kDa in wild-type cells, but not in *tat2*Δ cells, by immunoblot assay with affinity-purified antibodies, although some cross-reactive bands were also detected especially with the anti-N2 antibodies. In the following experiments, the anti-N1 antibodies were used if not otherwise specified.

The plasma membrane Tat2p level is regulated by extracellular tryptophan in the *trp1*Δ mutant as well as wild-type, and this is accomplished by rerouting intracellular transport of Tat2p (20). Because previous reports used strains expressing tagged Tat2 proteins, we reassessed the endogenous Tat2p level in cells grown in a different tryptophan concentration. In these assays, we first used *TRP1* strains rather than *trp1*Δ mutants to examine the effect of tryptophan depletion. Tat2p was most expressed when tryptophan was depleted from the medium (SDA-W) compared to the SDA medium with a low (30 μg/ml) or high (200 μg/ml) concentration of tryptophan (**Fig. 3*B***). We next examined intracellular localization of Tat2p by separating organelles on a sucrose density gradient. As shown in **Fig. 3*C***, the plasma membrane marker Pma1p fractionated in a denser fraction (#6), whereas the TGN marker Kex2p and the endosome marker Pep12p fractionated in lighter fractions (#3 and #4). Hereafter, the fraction #6 is referred to as the plasma membrane (PM)-rich fraction, whereas the fractions #3 and #4 are referred to as the internal membranes (IMs)-rich fraction. Tat2p was clearly increased in the PM-rich fraction by tryptophan depletion, whereas Tat2p in the IMs-rich fraction was little affected by extracellular tryptophan concentration (**Fig. 3*C***).

The fractionation profile of Tat2p was next examined in the *lem3*Δ and other mutants grown at 30°C. Tat2p in the PM-rich fraction was slightly decreased in the *lem3*Δ mutant, whereas it was clearly decreased in the *cho1*Δ mutant (**Fig. 3*D***). These results paralleled weak and strong tryptophan requirement in the *lem3*Δ *trp1*Δ and *cho1*Δ *trp1*Δ mutants, respectively (**Fig. 1*A***). In contrast, although the *fpk1*Δ *fpk2*Δ mutant exhibited strong tryptophan requirement (**Fig. 1*A***), Tat2p was only slightly decreased in this mutant, suggesting that the plasma membrane Tat2p might be less functional in the *fpk1*Δ *fpk2*Δ mutant. Tat2p in the PM-rich fraction was more decreased at 18°C in the *lem3*Δ and *fpk1*Δ *fpk2*Δ mutants (**Fig. 3*D***), again consistent with the growth phenotype (**Fig. 1*B***). The fractionation profile of Tat2p was also examined in the *lem3*Δ *trp1*Δ mutant grown in YPDA at 30°C, and it was confirmed that Tat2p was decreased in the PM-rich fraction (**Fig. 3*E***). These results suggest that the tryptophan requirement in the *lem3*Δ mutant is due to the decreased Tat2p in the plasma membrane. Tat2p that was not delivered to the plasma membrane seemed to be degraded, because the total cellular Tat2p level was decreased in the *lem3*Δ mutant

(**Fig. 3*F***). This reduction was suppressed by mutations in *PEP4* and *PRB1*, encoding vacuolar proteases that are required for maturation and activation of most vacuolar hydrolases (41,42). These results suggest that Tat2p is missorted to vacuoles in the *lem3*Δ mutant.

Tat2p may be missorted to the vacuole from the TGN in the lem3Δ mutant-Lem3p-Dnf1p and Lem3p-Dnf2p are recycled through the endocytic recycling pathway to maintain their primary localization to the plasma membrane (6,43,44). Thus, Lem3p-Dnf1/2p could regulate phospholipid asymmetry of endosomal/TGN membranes in addition to the plasma membrane. Two mechanisms can be envisioned to account for the decreased plasma membrane localization of Tat2p: (i) Tat2p is missorted to the vacuole from the TGN in the *lem3*Δ mutant, and (ii) Tat2p is rapidly endocytosed in the *lem3*Δ mutant. We first examined whether a mutation in genes involved in the vacuolar sorting pathway suppressed the tryptophan requirement in the *lem3*Δ mutant. The *VPS1* and *GGA1*/*GGA2* genes encode a dynamin-like GTPase (45,46) and Golgi-associated coat proteins with homology to gamma adaptin (47,48), respectively. Both proteins are implicated in vesicle formation from the TGN for transport to the vacuole via late endosomes. Thus, mutations in these genes would redeliver cargo proteins destined for the vacuole to the plasma membrane (46,49-51). As shown in **Fig 4*A***, both *vps1*Δ and *gga1*Δ *gga2*Δ mutations suppressed growth defects of the *lem3*Δ mutant on YPDA medium. If Tat2p is missorted to the vacuole through the vacuolar sorting pathway, mutations in late endosome-to-vacuole transport would also suppress the *lem3*Δ mutation. The *PEP12* and *VPS27* genes encode a t-SNARE required for vesicle fusion with late endosomes (52,53) and a subunit of the ESCRT-0 complex involved in the sorting of ubiquitinated cargo into intraluminal budding of the endosomal membrane (54-56), respectively. *pep12*Δ and *vps27*Δ mutations also suppressed growth defects of the *lem3*Δ mutant (**Fig. 4*A***).

We next confirmed that the suppression was caused by increased Tat2p at the plasma membrane. The PM-rich fraction was isolated by sucrose gradient centrifugation as described in **Fig. 3*C***, and Tat2p content was examined (**Fig. 4*B***). The *vps1*Δ mutation slightly increased Tat2p at the plasma membrane in the *lem3*Δ mutant, and the *gga1*Δ *gga2*Δ mutations substantially increased it, but to a lesser extent than the *pep12*Δ and *vps27*Δ mutations. In the *vps1*Δ and *gga1*Δ *gga2*Δ mutants, Tat2p might be transported to the vacuole via the TGN-to-early endosome pathway, which would not be affected by these mutations. As shown in **Fig. 4*C***, Dnf1p-GFP and Dnf2p-GFP were partially co-localized with a TGN marker Sec7p-mRFP (arrowheads) (57). Taken together, these results suggest that Tat2p is missorted to the vacuole from the TGN membrane whose phospholipid asymmetry is abnormally regulated in the *lem3*Δ mutant.

As shown in **Fig. 4*B***, the plasma membrane

Tat2p level in *pep12*Δ and *vps27*Δ mutants was not clearly decreased by the *lem3*Δ mutation, suggesting that Tat2p was not rapidly cleared from the plasma membrane by endocytosis in the *lem3*Δ mutant. In addition, Pomorski *et al*. reported that flippase mutants are rather defective in endocytosis: the uptake of a lipophilic dye FM4-64 was delayed in the *dnf1*Δ *dnf2*Δ mutant and the internalization of the mating factor receptor is inhibited in the *dnf1*Δ *dnf2*Δ *drs2*Δ mutant (14). If endocytosis of Tat2p is enhanced in the *lem3*Δ mutant, inhibition of endocytosis would recover Tat2p on the plasma membrane. *END3* and *VRP1* encode a factor of the endocytic coat/adaptor complex (58) and a regulator of cortical actin patch assembly (59), respectively, and removal of them cause a defect in receptor-mediated and fluid-phase endocytosis (60,61). However, to our great surprise, the *end3*Δ *trp1*Δ and *vrp1*Δ *trp1*Δ mutants exhibited tryptophan-dependent slow growth, which was suppressed by the overproduction of Tat2p (**Fig. 5*A***). Consistently, the plasma membrane Tat2p was decreased in these mutants as estimated by sucrose density gradient fractionation (**Fig. 5*B***). These results suggest that Tat2p is not properly delivered to the plasma membrane due to some indirect defect in the TGN-to-plasma membrane transport of Tat2p.

Lem3p-Dnf1p is recycled from the plasma membrane through early endosomes to the TGN and back to the plasma membrane (6,43). We previously showed that Dnf1p-GFP was exclusively localized to the plasma membrane in the *vrp1*Δ mutant (6). Similarly, Dnf1p-GFP and Dnf2p-GFP were localized to the plasma membrane in *end3*Δ cells (**Fig. 5*C***). Thus, in *end* mutants, Lem3p-Dnf1/2p could not be localized to the TGN, resulting in deregulated phospholipid asymmetry of this membrane. This would account for the possible missorting of Tat2p from the TGN to the vacuole in *end* mutants. Consistently, the *ypt6*Δ *trp1*Δ mutant, in which Dnf2p was mislocalized to endocytic recycling vesicles (62), also exhibited tryptophan requirement that was not strongly exacerbated by the additional *lem3*Δ mutation (**Fig. 5*D***). On the other hand, because various membrane proteins are recycled through the endocytic pathway, mislocalization of other proteins than Lem3p-Dnf1/2p may be also involved in the missorting of Tat2p.

Inhibition of ubiquitination restores plasma membrane localization of Tat2p-How does deregulated phospholipid asymmetry drive Tat2p to the vacuolar sorting pathway? Ubiquitination of yeast permeases is involved in their transport from the TGN to endosomes, endocytosis from the plasma membrane, and invagination into late endosomes (21). It was reported that ubiquitination at the TGN redirected Gap1p general amino acid permease to vacuoles from the exocytosis pathway (63). Thus we examined whether inhibition of Tat2p ubiquitination restored plasma membrane localization of Tat2p in the *lem3*Δ mutant. Beck *et al.* identified five lysine residues in the NH_2-terminal domain of Tat2p as

ubiquitin acceptor sites during starvation (22), and Umebayashi and Nakano reported that three (residues 10, 17, and 20) of them were mainly ubiquitinated (20). *TAT2*$^{3K>R}$, in which these three lysine residues were replaced by arginine, was constructed and the genomic *TAT2* was replaced with this allele. *TAT2*$^{3K>R}$ suppressed the tryptophan requirement in the *lem3*Δ *trp1*Δ mutant (**Fig. 6*A***). Rsp5p is an E3 ubiquitin ligase of the NEDD4 family and Bul1/2p are Rsp5p adaptors required for the substrate recognition (21). Both *bul1*Δ *bul2*Δ and *rsp5-1* mutations suppressed the tryptophan-dependent growth in the *lem3*Δ *trp1*Δ mutant (**Fig. 6*A***). To confirm that the plasma membrane localization of Tat2p was restored by inhibition of ubiquitination, the PM-rich fraction was isolated by sucrose gradient fractionation, and the Tat2p content was examined by immunoblotting. In these experiments, we used the anti-Tat2pN2 antibodies instead of the anti-Tat2pN1 antibodies, which were raised against the NH_2-terminal peptide containing the substitution sites of Tat2p$^{3K>R}$. All mutations increased the plasma membrane Tat2p in the *lem3*Δ mutant (**Fig. 6*B***). However, the increase by *TAT2*$^{3K>R}$ and *rsp5-1* mutations was not high, probably due to ubiquitination on other ubiquitin acceptor sites in Tat2p$^{3K>R}$ (e.g. residues 29 and 31) (22) and leakiness of the temperature-sensitive *rsp5-1* mutation at 30°C, respectively.

The results described above imply that Tat2p is ubiquitinated at the TGN and missorted to the vacuole in the *lem3*Δ mutant. However, we cannot exclude a possibility that the plasma membrane Tat2p was increased due to blockade of endocytosis. Interestingly, *TAT2*$^{3K>R}$ and *bul1*Δ also suppressed the tryptophan requirement in the *end3*Δ *trp1*Δ and *vrp1*Δ *trp1*Δ mutants (**Fig. 6*C***). These results suggest that ubiquitination of Tat2p occurs at the TGN, not at the plasma membrane, at least in *end* mutants. We also examined increased ubiquitination of Tat2p in the *lem3*Δ mutant. Tat2p was immunoprecipitated with the anti-Tat2p antibodies from cells expressing myc-tagged ubiquitin, followed by immunoblotting with the anti-myc antibody. However, we could not reproducibly detect an increase of ubiquitination in the *lem3*Δ mutant, because of abundant ubiquitinated Tat2p in wild-type cells, possibly originated from Tat2p localized in intracellular membranes (**Fig. 3*C*** and ***D***; our unpublished results).

Tryptophan import activity of Tat2p was not affected by the lem3Δ mutation-Since Lem3p-Dnf1/2p are implicated in phospholipid asymmetry in the plasma membrane (14,64), it is possible that tryptophan import activity of Tat2p is decreased by perturbed phospholipid asymmetry in the *lem3*Δ mutant. Tryptophan uptake was examined in the *lem3*Δ mutant using radiolabeled tryptophan. As shown in **Fig. 7*A***, tryptophan uptake was decreased in the *lem3*Δ mutant in accordance with the decreased Tat2 protein level in the PM-rich fraction (**Fig. 3*D***). Tat2p was mainly responsible for this tryptophan uptake in the *lem3*Δ mutant as well as in the wild type. To

compare the Tat2p activity more precisely between the wild type and *lem3*Δ mutant, we constructed a *lem3*Δ mutant that expressed Tat2p at the plasma membrane in a level comparable to that in the wild type by transforming the *lem3*Δ mutant with YCp-TAT2. The plasma membrane Tat2p level in this strain was 129 ± 15% of the wild type. As shown in **Fig. 7*B***, tryptophan uptake was not affected by the *lem3*Δ mutation when the Tat2p level in the *lem3*Δ mutant was normalized to the wild type. These results suggest that tryptophan requirement in the *lem3*Δ mutant is not caused by decreased Tat2p activity.

Interaction of the Tat2p NH_2-terminal cytoplasmic region with phosphatidylserine may be involved in the ubiquitination of Tat2p-We next investigated a mechanism for sensing perturbed phospholipid asymmetry by Tat2p. If Tat2p is directly involved in the sensing, the sensing site might be located in the vicinity of the ubiquitination sites in the NH_2-terminal region. Thus, we examined whether the Tat2p NH_2-terminal region (residues 1-85, Tat2pNT) directly interacted with phospholipids by the liposome flotation assay (35). In these experiments, liposomes and their bound proteins move to the top (T) fraction from the bottom (B) fraction after centrifugation, whereas unbound proteins are left in the bottom fraction. Interestingly, GST-Tat2pNT bound to liposomes composed of 80% DOPC and 20% DOPS, or 80% DOPC and 20% PA (mol/mol) (**Fig. 8*A***). GST-Tat2pNT very weakly bound to 80% DOPC and 20% PI liposomes, but did not bind to DOPC-only liposomes or 80% DOPC and 20% DOPE liposomes, suggesting that GST-Tat2pNT specifically bound to acidic phospholipid-containing liposomes in a manner that PS and PA are preferable. These results are interesting, because Lem3p-Dnf1/2p are suggested to translocate PS but not PA to the cytoplasmic leaflet (14) (see DISCUSSION).

To evaluate the physiological significance of the above findings, we isolated mutant Tat2pNT proteins that were impaired in the binding to PS-containing liposomes. Given that the interaction was sensitive to high salt concentrations (e.g. 200 mM KCl; our unpublished results), we speculated that positively-charged amino acids may be involved in the lipid binding. The partial amino acid sequence of Tat2pNT is shown in **Fig. 8*B***. This region is highly variable among yeast amino acid permeases except conserved sequence (residues 78-85) that precedes the first transmembrane domain. Two lysine- and arginine-containing sequences, regions 1 and 2, which are separated by a serine-rich sequence (residues 34-47) were found. In the region 1, five lysine residues (10, 17, 20, 29, and 31) had been identified as ubiquitin acceptor lysines (22), and these lysines were replaced with alanines to construct $Tat2pNT^{5K>A}$. There are also two arginine residues (11 and 19) in this region, and they were replaced with alanines to construct $Tat2pNT^{2R>A}$. In the region 2, there are two arginine residues (55 and 60) and lysine residues (54 and 66), and these four residues were replaced

with alanines to construct Tat2pNT$^{2K2R>A}$. These three mutant proteins fused to GST were expressed and purified, and were examined for binding to the PC liposomes containing 20% PS (**Fig. 8*C***). Interestingly, the 2K2R>A substitutions greatly impaired the interaction: only 14.8 ± 1.1% of GST-Tat2pNT$^{2K2R>A}$ was found in the top fraction compared to 71.2 ± 4.5% of the wild type. The binding of GST-Tat2pNT$^{5K>A}$ was slightly impaired to 42.4 ± 9.6%, but that of GST-Tat2pNT$^{2R>A}$ was not affected. These results suggest that the four basic residues in the region 2 are mainly involved in the PS-liposome binding.

We next constructed mutant *tat2* genes containing these substitutions and expressed them in the *tat2*Δ *trp1*Δ mutant. Most interestingly, the *tat2*$^{2K2R>A}$ gene failed to complement the *tat2*Δ mutation (**Fig. 8*D***). This was because the plasma membrane Tat2p$^{2K2R>A}$ was decreased as estimated by sucrose gradient fractionation (**Fig. 8*E***). We next expressed the *tat2*$^{2K2R>A}$ gene in the *bul1*Δ *bul2*Δ *tat2*Δ *trp1*Δ mutant. As shown in **Fig. 8*F***, *bul1*Δ *bul2*Δ mutations clearly suppressed the tryptophan requirement of the *tat2*$^{2K2R>A}$ mutant. Taken together, these results suggest that Tat2p$^{2K2R>A}$ is ubiquitinated and missorted to the vacuole, possibly because its NH_2-terminal region does not interact with membranes.

We similarly examined the functionality of *TAT2*$^{5K>A}$ and *TAT2*$^{2R>A}$ mutant genes. The *TAT2*$^{5K>A}$ mutation restored growth in the *lem3*Δ *tat2*Δ *trp1*Δ mutant as well as in the *tat2*Δ *trp1*Δ mutant (**Fig. 8*D***), consistent with the previous observation that the mutated lysine residues are ubiquitin acceptor sites: this protein would be continuously transported to the plasma membrane from the TGN and would be defective in its endocytosis (22,65). In fact, Tat2p$^{5K>A}$ was exclusively found in the PM-rich fraction (**Fig. 8*E***). As shown in **Fig. 8*C***, GST-Tat2pNT$^{5K>A}$ exhibited a ~30% reduction in liposome binding. It is an interesting possibility that these lysine residues are also involved in sensing the PS level for ubiquitination of Tat2p. The *TAT2*$^{2R>A}$ mutant behaved like wild type in tryptophan requirement for growth and subcellular localization (**Fig. 8*D*** and ***E***). Consistently, this mutation did not affect the binding to PS-containing liposomes (**Fig. 8*C***).

DISCUSSION

Here we report that phospholipid flippases Lem3p-Dnf1/2p are involved in the plasma membrane localization of Tat2p. Considering the primary localization site of Lem3p-Dnf1/2p at the plasma membrane, we first speculated that the missorting of Tat2p was due to the perturbation of phospholipid asymmetry at the plasma membrane. However, the missorting seems to occur at the TGN, because the inhibition of TGN-to-late endosome transport rerouted Tat2p to the plasma membrane. Interestingly, endocytosis-defective mutants also exhibited the defects in the plasma membrane localization of Tat2p, suggesting that, in *end* mutants, Tat2p was also missorted from the TGN to the vacuole. In *end* mutants, various membrane proteins that are recycled through the

endocytic pathway are trapped at the plasma membrane. Thus, the Tat2p missorting seems to be caused by sequestering some proteins including Lem3p-Dnf1/2p from the TGN. Consistently, the *end3*Δ mutation did not exhibit a synthetic tryptophan requirement with the *lem3*Δ *trp1*Δ mutations at 25°C (our unpublished results). Although we cannot exclude a possibility that Tat2p is endocytosed at an increased rate in the *lem3*Δ mutant, it is not plausible, because (i) the plasma membrane-associated Tat2p level was not very different between *pep12*Δ and *lem3*Δ *pep12*Δ mutants (**Fig. 4*B***), and (ii) Lem3p-Dnf1/2p were rather required for endocytosis (14).

If phospholipid flip at the TGN is generally required for the plasma membrane transport of Tat2p, the *cdc50*Δ/*drs2*Δ *trp1*Δ mutant should exhibit stronger tryptophan requirement, because Cdc50p-Drs2p is mainly localized to TGN/endosomal membranes (13). However, the *cdc50*Δ/*drs2*Δ mutants exhibited weaker tryptophan requirement than the *lem3*Δ/*dnf1/2*Δ mutants, taking into account slower growth rates of the *cdc50*Δ/*drs2*Δ mutants in tryptophan-rich medium (**Fig. 1*A***). One possibility is that Lem3p-Dnf1/2p and Tat2p are present in similar membrane microenvironment: both proteins have been reported to be present in detergent resistant membrane domains so called lipid rafts (20,64). In yeast, most plasma membrane proteins including Lem3p and Tat2p were found to be associated with lipid rafts. Accumulating evidence suggests that lipid rafts function as a sorting platform at the TGN for cell surface delivery of plasma membrane proteins (66). Quantitative analysis of isolated secretory vesicles by mass spectrometry revealed that they are highly enriched in ergosterol and sphingolipids compared to the donor TGN membranes (67). Thus, Lem3p-Dnf1/2p and Tat2p may be segregated at the TGN from Cdc50p-Drs2p, which is normally transported to the early endosome. It is unknown how phospholipid asymmetry is organized in these raft domains, but Lem3p-Dnf1/2p may affect the destination of Tat2p by flipping phospholipids in raft domains.

The binding of Tat2pNT to liposomes required positively charged amino acid residues and PS or PA on liposomes, suggesting that the NH_2-terminal region of Tat2p electrostatically interacts with negatively charged membranes. It was reported that the *trp1*Δ mutant exhibited growth sensitivity to weak organic acid stress, which was suppressed by tryptophan supplementation or overexpression of Tat2p (68). Acid stress might disrupt the electrostatic interaction of Tat2p with membranes, resulting in mislocalization of Tat2p. Electrostatic interaction between a cytoplasmic region and membranes is involved in the regulation of various membrane proteins. The cytoplasmic C-terminal domain of the epithelial Na^+/H^+ exchanger NHE3 interacted with negatively-charged membranes through basic residues, and this association seemed to be involved in the regulation of NHE3 activity *in vivo* (69). In rhodopsin, a cytoplasmic helical segment

(H8) extending from the transmembrane domain seven could act as a membrane-dependent conformational switch by interacting with PS (70). In addition, it has been proposed that a cytoplasmic juxtamembrane domain of epidermal growth factor receptor binds electrostatically to acidic phospholipids in the plasma membrane, resulting in autoinhibition of the tyrosine kinase activity (71).

It has not been clearly demonstrated that Lem3p-Dnf1/2p flip PS, because (i) NBD-labeled PS was still flipped in the *lem3*Δ mutant probably due to an unidentified protein on the plasma membrane (72), and (ii) NBD-PS was a less preferred substrate of Dnf1p compared to NBD-PC and NBD-PE (73). However, growth of the *lem3*Δ mutant was clearly sensitive to papuamide B, a cyclic lipopeptide that shows cytotoxicity by binding to PS in biological membranes (74), and this sensitivity was suppressed by the *cho1*Δ mutation (our unpublished results), indicating that PS is exposed on the cell surface in this mutant. These results may suggest that Lem3p-Dnf1/2p flips PS more efficiently than NBD-PS. The results that Tat2p was missorted in the *cho1*Δ mutant (**Fig. 3*D***) also support that PS is involved in Tat2p transport. Involvement of PS was also demonstrated for the ferrichrome-induced plasma membrane transport of the siderophore transporter Arn1p: Arn1p-GFP was mislocalized to intracellular structures in the *cho1*Δ mutant (75). Interestingly, in the *drs2*Δ mutant, the ferrichrome-induced plasma membrane transport of Arn1p-GFP was not affected, whereas Arn1p-GFP was mislocalized to the plasma membrane in the absence of ferrichrome. It seems that phospholipid asymmetry is involved in sorting of various membrane proteins in a different manner.

Because it was suggested that Lem3p-Dnf1/2p flip PE and PC (14,64), these phospholipids may be also involved in Tat2p missorting. Interaction with the Tat2p NH_2-terminal region was not detected with PE or PC in the liposome flotation experiments, but it is possible that changes in asymmetric distribution of these lipids are sensed through other regions of Tat2p or by other proteins that regulate Tat2p ubiquitination. Further studies are required to examine these possibilities.

Inhibition of ubiquitination restored plasma membrane localization of Tat2p in the *lem3*Δ mutant, suggesting that perturbation of phospholipid asymmetry induces ubiquitination of Tat2p. Thus, an important question is how changes in phospholipid asymmetry are sensed and ultimately result in ubiquitination of Tat2p. Identification of the liposome-binding activity in the Tat2p NH_2-terminal region shed light on this mechanism. Amino acid substitutions that reduced interaction with liposomes (2K2R>A: K54A, R55A, R60A, and K66A) caused ubiquitination-dependent missorting of Tat2p. These results suggest that $Tat2p^{2K2R>A}$ mimics Tat2p in the *lem3*Δ mutant, although we cannot exclude a possibility that the substitutions cause

other defects such as structural change or inability to interact with an interacting protein. Since these residues are close to the ubiquitin acceptor lysines (residues 10, 17, 20, 29, and 31), we propose that the interaction of the Tat2p NH_2-terminal region with PS/PA-rich membranes through the basic residues plays an important role for whether Tat2p is ubiquitinated or not. When the Tat2p NH_2-terminal region is bound to membrane phospholipids, it is not ubiquitinated, but when it dissociates from the membrane, Tat2p would be ubiquitinated and then transported to the vacuole. To test this hypothesis, ubiquitination of Tat2p should be reconstituted *in vitro* with liposomes. PA, which seems not to be flipped by Lem3p-Dnf1/2p (14), is likely to exist in TGN/endosomal membranes at a level comparable to that of PS (67). This might account for the mild missorting of Tat2p in the *lem3*Δ mutant.

Plasma membrane localization of Tat2p is also sensitive to perturbation of other lipids, including ergosterol: Tat2p was missorted to the vacuole by ubiquitination in the *erg6*Δ mutant (20). Thus, Tat2p is suitable for the study of effects of lipid microenvironment on protein sorting.

REFERENCES

1. Devaux, P. F., López-Montero, I., and Bryde, S. (2006) Proteins involved in lipid translocation in eukaryotic cells. *Chem Phys Lipids* **141**, 119-132

2. Daleke, D. L. (2007) Phospholipid flippases. *J Biol Chem* **282**, 821-825

3. Lenoir, G., Williamson, P., and Holthuis, J. C. (2007) On the origin of lipid asymmetry: the flip side of ion transport. *Curr Opin Chem Biol* **11**, 654-661

4. Tanaka, K., Fujimura-Kamada, K., and Yamamoto, T. (2011) Functions of phospholipid flippases. *J Biochem* **149**, 131-143

5. Sebastian, T. T., Baldridge, R. D., Xu, P., and Graham, T. R. (2012) Phospholipid flippases: Building asymmetric membranes and transport vesicles. *Biochim Biophys Acta* **1821**, 1068-1077

6. Saito, K., Fujimura-Kamada, K., Furuta, N., Kato, U., Umeda, M., and Tanaka, K. (2004) Cdc50p, a protein required for polarized growth, associates with the Drs2p P-type ATPase implicated in phospholipid translocation in *Saccharomyces cerevisiae*. *Mol Biol Cell* **15**, 3418-3432

7. Furuta, N., Fujimura-Kamada, K., Saito, K., Yamamoto, T., and Tanaka, K. (2007) Endocytic recycling in yeast is regulated by putative phospholipid translocases and the Ypt31p/32p-Rcy1p pathway. *Mol Biol Cell* **18**, 295-312

8. Lenoir, G., Williamson, P., Puts, C. F., and Holthuis, J. C. (2009) Cdc50p plays a vital role in the ATPase reaction cycle of the putative aminophospholipid transporter Drs2p. *J Biol Chem* **284**, 17956-17967

9. Takahashi, Y., Fujimura-Kamada, K., Kondo, S., and Tanaka, K. (2011) Isolation and characterization of novel mutations in *CDC50*, the non-catalytic subunit of the Drs2p phospholipid flippase. *J Biochem* **149**, 423-432

10. Jacquot, A., Montigny, C., Hennrich, H., Barry, R., le Maire, M., Jaxel, C., Holthuis, J., Champeil, P., and Lenoir, G. (2012) Phosphatidylserine stimulation of Drs2p·Cdc50p lipid translocase dephosphorylation is controlled by phosphatidylinositol-4-phosphate. *J Biol Chem* **287**, 13249-13261

11. Natarajan, P., Wang, J., Hua, Z., and Graham, T. R. (2004) Drs2p-coupled aminophospholipid translocase activity in yeast Golgi membranes and relationship to *in vivo* function. *Proc Natl Acad Sci U S A* **101**, 10614-10619

12. Alder-Baerens, N., Lisman, Q., Luong, L., Pomorski, T., and Holthuis, J. C. (2006) Loss of P4 ATPases Drs2p and Dnf3p disrupts aminophospholipid transport and asymmetry in yeast post-Golgi secretory vesicles. *Mol Biol Cell* **17**, 1632-1642

13. Hua, Z., Fatheddin, P., and Graham, T. R. (2002) An essential subfamily of Drs2p-related P-type ATPases is required for protein trafficking between Golgi complex and endosomal/vacuolar system. *Mol Biol Cell* **13**, 3162-3177

14. Pomorski, T., Lombardi, R., Riezman, H., Devaux, P. F., van Meer, G., and Holthuis, J. C. (2003) Drs2p-related P-type ATPases Dnf1p and Dnf2p are required for phospholipid translocation across the yeast plasma membrane and serve a role in endocytosis. *Mol Biol Cell* **14**, 1240-1254

15. Nakano, K., Yamamoto, T., Kishimoto, T., Noji, T., and Tanaka, K. (2008) Protein kinases Fpk1p and Fpk2p are novel regulators of phospholipid asymmetry. *Mol Biol Cell* **19**, 1783-1797

16. Devaux, P. F., Herrmann, A., Ohlwein, N., and Kozlov, M. M. (2008) How lipid flippases can modulate membrane structure. *Biochim Biophys Acta* **1778**, 1591-1600

17. Graham, T. R., and Kozlov, M. M. (2010) Interplay of proteins and lipids in generating membrane curvature. *Curr Opin Cell Biol* **22**, 430-436

18. Saito, K., Fujimura-Kamada, K., Hanamatsu, H., Kato, U., Umeda, M., Kozminski, K. G., and Tanaka, K. (2007) Transbilayer phospholipid flipping regulates Cdc42p signaling during polarized cell growth via Rga GTPase-activating proteins. *Dev Cell* **13**, 743-751

19. Das, A., Slaughter, B. D., Unruh, J. R., Bradford, W. D., Alexander, R., Rubinstein, B., and Li, R. (2012) Flippase-mediated phospholipid asymmetry promotes fast Cdc42 recycling in dynamic maintenance of cell polarity. *Nat Cell Biol* **14**, 304-310

20. Umebayashi, K., and Nakano, A. (2003) Ergosterol is required for targeting of tryptophan permease to the yeast plasma membrane. *J Cell Biol* **161**, 1117-1131

21. Lauwers, E., Erpapazoglou, Z., Haguenauer-Tsapis, R., and André, B. (2010) The ubiquitin code of yeast permease trafficking. *Trends Cell Biol* **20**, 196-204

22. Beck, T., Schmidt, A., and Hall, M. (1999) Starvation induces vacuolar targeting and degradation of the tryptophan permease in yeast. *J Cell Biol* **146**, 1227-1238

23. Nakamura, H., Miura, K., Fukuda, Y., Shibuya, I., Ohta, A., and Takagi, M. (2000) Phosphatidylserine synthesis required for the maximal tryptophan transport activity in *Saccharomyces cerevisiae*. *Biosci Biotechnol Biochem* **64**, 167-172

24. Rodríguez-Vargas, S., Sánchez-García, A., Martínez-Rivas, J. M., Prieto, J. A., and Randez-Gil, F. (2007) Fluidization of membrane lipids enhances the tolerance of *Saccharomyces cerevisiae* to freezing and salt stress. *Appl Environ Microbiol* **73**, 110-116

25. Rose, M. D., Winston, F., and Hieter, P. (1990) *Methods in Yeast Genetics: A Laboratory Course Manual*, Cold Spring Harbor Laboratory Press, Cold Spring Harbor, NY

26. Guthrie, C., and Fink, G. R., eds. (1991) *Guide to yeast genetics and molecular biology*. *Methods Enzymology* **350**, Academic Press, San Diego

27. Elble, R. (1992) A simple and efficient procedure for transformation of yeasts. *Biotechniques* **13**, 18-20

28. Gietz, R. D., and Woods, R. A. (2002) Transformation of yeast by lithium acetate/single-stranded carrier DNA/polyethylene glycol method. *Methods Enzymol* **350**, 87-96

29. Brachmann, C. B., Davies, A., Cost, G. J., Caputo, E., Li, J., Hieter, P., and Boeke, J. D. (1998) Designer deletion strains derived from *Saccharomyces cerevisiae* S288C: a useful set of strains and plasmids for PCR-mediated gene disruption and other applications. *Yeast* **14**, 115-132

30. Longtine, M. S., McKenzie, A., Demarini, D. J., Shah, N. G., Wach, A., Brachat, A., Philippsen, P., and Pringle, J. R. (1998) Additional modules for versatile and economical PCR-based gene deletion and modification in *Saccharomyces cerevisiae*. *Yeast* **14**, 953-961

31. Goldstein, A. L., and McCusker, J. H. (1999) Three new dominant drug resistance cassettes for gene disruption in *Saccharomyces cerevisiae*. *Yeast* **15**, 1541-1553

32. Ho, S. N., Hunt, H. D., Horton, R. M., Pullen, J. K., and Pease, L. R. (1989) Site-directed mutagenesis by overlap extension using the polymerase chain reaction. *Gene* **77**, 51-59

33. Valdivia, R. H., and Schekman, R. (2003) The yeasts Rho1p and Pkc1p regulate the transport of chitin synthase III (Chs3p) from internal stores to the plasma membrane. *Proc Natl Acad Sci U S A* **100**, 10287-10292

34. Misu, K., Fujimura-Kamada, K., Ueda, T., Nakano, A., Katoh, H., and Tanaka, K. (2003) Cdc50p, a conserved endosomal membrane protein, controls polarized growth in *Saccharomyces cerevisiae*. *Mol Biol Cell* **14**, 730-747

35. Bigay, J., Casella, J. F., Drin, G., Mesmin, B., and Antonny, B. (2005) ArfGAP1 responds to membrane curvature through the folding of a lipid packing sensor motif. *EMBO J* **24**, 2244-2253

36. Heitman, J., Koller, A., Kunz, J., Henriquez, R., Schmidt, A., Movva, N. R., and Hall, M. N. (1993) The immunosuppressant FK506 inhibits amino acid import in *Saccharomyces cerevisiae*. *Mol Cell Biol* **13**, 5010-5019

37. Mochida, J., Yamamoto, T., Fujimura-Kamada, K., and Tanaka, K. (2002) The novel adaptor protein, Mti1p, and Vrp1p, a homolog of Wiskott-Aldrich syndrome protein-interacting protein (WIP), may antagonistically regulate type I myosins in *Saccharomyces cerevisiae*. *Genetics* **160**, 923-934

38. Braus, G. H. (1991) Aromatic amino acid biosynthesis in the yeast *Saccharomyces cerevisiae*: a model system for the regulation of a eukaryotic biosynthetic pathway. *Microbiol Rev* **55**, 349-370

39. Schmidt, A., Hall, M., and Koller, A. (1994) Two FK506 resistance-conferring genes in *Saccharomyces cerevisiae*, *TAT1* and *TAT2*, encode amino acid permeases mediating tyrosine and tryptophan uptake. *Mol Cell Biol* **14**, 6597-6606

40. Roelants, F. M., Baltz, A. G., Trott, A. E., Fereres, S., and Thorner, J. (2010) A protein kinase network regulates the function of aminophospholipid flippases. *Proc Natl Acad Sci U S A* **107**, 34-39

41. Zubenko, G. S., Park, F. J., and Jones, E. W. (1982) Genetic properties of mutations at the *PEP4* locus in *Saccharomyces cerevisiae*. *Genetics* **102**, 679-690

42. Jones, E. W., Zubenko, G. S., and Parker, R. R. (1982) *PEP4* gene function is required for expression of several vacuolar hydrolases in *Saccharomyces cerevisiae*. *Genetics* **102**, 665-677

43. Liu, K., Hua, Z., Nepute, J. A., and Graham, T. R. (2007) Yeast P4-ATPases Drs2p and Dnf1p are essential cargos of the NPFXD/Sla1p endocytic pathway. *Mol Biol Cell* **18**, 487-500

44. Takagi, K., Iwamoto, K., Kobayashi, S., Horiuchi, H., Fukuda, R., and Ohta, A. (2011) Involvement of Golgi-associated retrograde protein complex in the recycling of the putative Dnf aminophospholipid flippases in yeast. *Biochem Biophys Res Commun*

45. Vater, C. A., Raymond, C. K., Ekena, K., Howald-Stevenson, I., and Stevens, T. H. (1992) The *VPS1* protein, a homolog of dynamin required for vacuolar protein sorting in *Saccharomyces cerevisiae*, is a GTPase with two functionally separable domains. *J Cell Biol* **119**, 773-786

46. Bensen, E. S., Costaguta, G., and Payne, G. S. (2000) Synthetic genetic interactions with temperature-sensitive clathrin in *Saccharomyces cerevisiae*. Roles for synaptojanin-like Inp53p and dynamin-related Vps1p in clathrin-dependent protein sorting at the *trans*-Golgi network. *Genetics* **154**, 83-97

47. Dell'Angelica, E. C., Puertollano, R., Mullins, C., Aguilar, R. C., Vargas, J. D., Hartnell, L. M., and Bonifacino, J. S. (2000) GGAs: a family of ADP ribosylation factor-binding proteins related to adaptors and associated with the Golgi complex. *J Cell Biol* **149**, 81-94

48. Hirst, J., Lui, W. W., Bright, N. A., Totty, N., Seaman, M. N., and Robinson, M. S. (2000) A family of proteins with gamma-adaptin and VHS domains that facilitate trafficking between the *trans*-Golgi network and the vacuole/lysosome. *J Cell Biol* **149**, 67-80

49. Nothwehr, S. F., Conibear, E., and Stevens, T. H. (1995) Golgi and vacuolar membrane proteins reach the vacuole in *vps1* mutant yeast cells via the plasma membrane. *J Cell Biol* **129**, 35-46

50. Costaguta, G., Stefan, C. J., Bensen, E. S., Emr, S. D., and Payne, G. S. (2001) Yeast Gga coat proteins function with clathrin in Golgi to endosome transport. *Mol Biol Cell* **12**, 1885-1896

51. Scott, P. M., Bilodeau, P. S., Zhdankina, O., Winistorfer, S. C., Hauglund, M. J., Allaman, M. M., Kearney, W. R., Robertson, A. D., Boman, A. L., and Piper, R. C. (2004) GGA proteins bind ubiquitin to facilitate sorting at the *trans*-Golgi network. *Nat Cell Biol* **6**, 252-259

52. Gerrard, S. R., Levi, B. P., and Stevens, T. H. (2000) Pep12p is a multifunctional yeast syntaxin that controls entry of biosynthetic, endocytic and retrograde traffic into the prevacuolar compartment. *Traffic* **1**, 259-269

53. Becherer, K. A., Rieder, S. E., Emr, S. D., and Jones, E. W. (1996) Novel syntaxin homologue, Pep12p, required for the sorting of lumenal hydrolases to the lysosome-like vacuole in yeast. *Mol Biol Cell* **7**, 579-594

54. Bilodeau, P. S., Winistorfer, S. C., Kearney, W. R., Robertson, A. D., and Piper, R. C. (2003) Vps27-Hse1 and ESCRT-I complexes cooperate to increase efficiency of sorting ubiquitinated proteins at the endosome. *J Cell Biol* **163**, 237-243

55. Piper, R. C., Cooper, A. A., Yang, H., and Stevens, T. H. (1995) *VPS27* controls vacuolar and endocytic traffic through a prevacuolar compartment in *Saccharomyces cerevisiae*. *J Cell Biol* **131**, 603-617

56. Katzmann, D. J., Stefan, C. J., Babst, M., and Emr, S. D. (2003) Vps27 recruits ESCRT machinery to endosomes during MVB sorting. *J Cell Biol* **162**, 413-423

57. Franzusoff, A., Redding, K., Crosby, J., Fuller, R. S., and Schekman, R. (1991) Localization of components involved in protein transport and processing through the yeast Golgi apparatus. *J Cell Biol* **112**, 27-37

58. Tang, H. Y., Munn, A., and Cai, M. (1997) EH domain proteins Pan1p and End3p are components of a complex that plays a dual role in organization of the cortical actin cytoskeleton and endocytosis in *Saccharomyces cerevisiae*. *Mol Cell Biol* **17**, 4294-4304

59. Vaduva, G., Martin, N. C., and Hopper, A. K. (1997) Actin-binding verprolin is a polarity development protein required for the morphogenesis and function of the yeast actin cytoskeleton. *J Cell Biol* **139**, 1821-1833

60. Raths, S., Rohrer, J., Crausaz, F., and Riezman, H. (1993) *end3* and *end4*: two mutants defective in receptor-mediated and fluid-phase endocytosis in *Saccharomyces cerevisiae*. *J Cell Biol* **120**, 55-65

61. Munn, A. L., Stevenson, B. J., Geli, M. I., and Riezman, H. (1995) *end5*, *end6*, and *end7*: mutations that cause actin delocalization and block the internalization step of endocytosis in *Saccharomyces cerevisiae*. *Mol Biol Cell* **6**, 1721-1742

62. Takagi, K., Iwamoto, K., Kobayashi, S., Horiuchi, H., Fukuda, R., and Ohta, A. (2012) Involvement of Golgi-associated retrograde protein complex in the recycling of the putative Dnf aminophospholipid flippases in yeast. *Biochem Biophys Res Commun* **417**, 490-494

63. Risinger, A. L., and Kaiser, C. A. (2008) Different ubiquitin signals act at the Golgi and plasma membrane to direct *GAP1* trafficking. *Mol Biol Cell* **19**, 2962-2972

64. Kato, U., Emoto, K., Fredriksson, C., Nakamura, H., Ohta, A., Kobayashi, T., Murakami-Murofushi, K., and Umeda, M. (2002) A novel membrane protein, Ros3p, is required for phospholipid translocation across the plasma membrane in *Saccharomyces cerevisiae*. *J Biol Chem* **277**, 37855-37862

65. Nagayama, A., Kato, C., and Abe, F. (2004) The N- and C-terminal mutations in tryptophan permease Tat2 confer cell growth in *Saccharomyces cerevisiae* under high-pressure and low-temperature conditions. *Extremophiles* **8**, 143-149

66. Surma, M. A., Klose, C., and Simons, K. (2012) Lipid-dependent protein sorting at the *trans*-Golgi network. *Biochim Biophys Acta* **1821**, 1059-1067

67. Klemm, R. W., Ejsing, C. S., Surma, M. A., Kaiser, H. J., Gerl, M. J., Sampaio, J. L., de Robillard, Q., Ferguson, C., Proszynski, T. J., Shevchenko, A., and Simons, K. (2009) Segregation of sphingolipids and sterols during formation of secretory vesicles at the *trans*-Golgi network. *J Cell Biol* **185**, 601-612

68. Bauer, B., Rossington, D., Mollapour, M., Mamnun, Y., Kuchler, K., and Piper, P. (2003) Weak organic acid stress inhibits aromatic amino acid uptake by yeast, causing a strong influence of

amino acid auxotrophies on the phenotypes of membrane transporter mutants. *Eur J Biochem* **270**, 3189-3195

69. Alexander, R. T., Jaumouillé, V., Yeung, T., Furuya, W., Peltekova, I., Boucher, A., Zasloff, M., Orlowski, J., and Grinstein, S. (2011) Membrane surface charge dictates the structure and function of the epithelial Na^+/H^+ exchanger. *EMBO J* **30**, 679-691

70. Krishna, A. G., Menon, S. T., Terry, T. J., and Sakmar, T. P. (2002) Evidence that helix 8 of rhodopsin acts as a membrane-dependent conformational switch. *Biochemistry* **41**, 8298-8309

71. McLaughlin, S., Smith, S. O., Hayman, M. J., and Murray, D. (2005) An electrostatic engine model for autoinhibition and activation of the epidermal growth factor receptor (EGFR/ErbB) family. *J Gen Physiol* **126**, 41-53

72. Stevens, H. C., Malone, L., and Nichols, J. W. (2008) The putative aminophospholipid translocases, *DNF1* and *DNF2*, are not required for 7-nitrobenz-2-oxa-1,3-diazol-4-yl-phosphatidylserine flip across the plasma membrane of *Saccharomyces cerevisiae*. *J Biol Chem* **283**, 35060-35069

73. Baldridge, R. D., and Graham, T. R. (2012) Identification of residues defining phospholipid flippase substrate specificity of type IV P-type ATPases. *Proc Natl Acad Sci U S A* **109**, E290-298

74. Parsons, A. B., Lopez, A., Givoni, I. E., Williams, D. E., Gray, C. A., Porter, J., Chua, G., Sopko, R., Brost, R. L., Ho, C. H., Wang, J., Ketela, T., Brenner, C., Brill, J. A., Fernandez, G. E., Lorenz, T. C., Payne, G. S., Ishihara, S., Ohya, Y., Andrews, B., Hughes, T. R., Frey, B. J., Graham, T. R., Andersen, R. J., and Boone, C. (2006) Exploring the mode-of-action of bioactive compounds by chemical-genetic profiling in yeast. *Cell* **126**, 611-625

75. Guo, Y., Au, W. C., Shakoury-Elizeh, M., Protchenko, O., Basrai, M., Prinz, W. A., and Philpott, C. C. (2010) Phosphatidylserine is involved in the ferrichrome-induced plasma membrane trafficking of Arn1 in *Saccharomyces cerevisiae*. *J Biol Chem* **285**, 39564-39573

76. Gietz, R. D., and Sugino, A. (1988) New yeast-*Escherichia coli* shuttle vectors constructed with *in vitro* mutagenized yeast genes lacking six-base pair restriction sites. *Gene* **74**, 527-534

77. Kikyo, M., Tanaka, K., Kamei, T., Ozaki, K., Fujiwara, T., Inoue, E., Takita, Y., Ohya, Y., and Takai, Y. (1999) An FH domain-containing Bnr1p is a multifunctional protein interacting with a variety of cytoskeletal proteins in *Saccharomyces cerevisiae*. *Oncogene* **18**, 7046-7054

78. Abe, F., and Iida, H. (2003) Pressure-induced differential regulation of the two tryptophan permeases Tat1 and Tat2 by ubiquitin ligase Rsp5 and its binding proteins, Bul1 and Bul2. *Mol Cell Biol* **23**, 7566-7584

79. Abe, F., and Horikoshi, K. (2000) Tryptophan permease gene *TAT2* confers high-pressure growth in *Saccharomyces cerevisiae*. *Mol Cell Biol* **20**, 8093-8102

Acknowledgements—*We thank Drs. Akihiko Nakano, Fumiyoshi Abe, Ramon Serrano, and Steven Nothwehr for yeast strains, plasmids, and antibodies. We thank Tomohiro Hirose in Instrumental Analysis Division, Equipment Management Center, Creative Research Institution, Hokkaido University for amino acid compositional analysis. We thank our colleagues in the Tanaka laboratory for valuable discussions and Eriko Itoh for technical assistance.*

FOOTNOTES

[*]This work was supported by JSPS KAKENHI Grant number 21570192 and 21370085.

[1]To whom correspondence should be addressed: Kazuma Tanaka, Division of Molecular Interaction, Institute for Genetic Medicine, Hokkaido University Graduate School of Life Science, N15 W7, Kita-ku, Sapporo, 060-0815, Japan. Tel.: +81–11–706–5165; Fax: +81–11–706–7821; E-mail: k-tanaka@igm.hokudai.ac.jp.

[2]The abbreviations used are: PC, phosphatidylcholine; PE, phosphatidylethanolamine; PS, phosphatidylserine; P4-ATPase, type 4 P-type ATPase; TGN, *trans*-Golgi network; mRFP, monomeric red fluorescent protein 1; Tat2pNT, NH_2-terminal cytoplasmic region (residues 1-85) of Tat2p; DOPC, dioleoylphosphatidylcholine; DOPE, dioleoylphosphatidylethanolamine; DOPS, dioleoylphosphatidylserine; PA, phosphatidic acid; PI phosphatidylinositol; NBD, 7-nitrobens-2-oxa-1,3-diazol-4-yl; PM, plasma membrane; IMs, internal membranes.

FIGURE LEGENDS

FIGURE 1. **The *lem3*Δ *trp1*Δ mutant exhibits tryptophan-dependent growth.** *A* and *B*, Tryptophan requirement in flippase and flippase-related mutants. Cells were grown to early log phase in YPDAW, washed, and adjusted at a concentration of 2.5 x 10^7 cells/ml. 4 μl drops of five-fold serial dilutions were spotted on YPDAW or YPDA, followed by incubation at 30°C for 20 hours (*A*) or at 18°C for 3 days (*B*). Strains were KKT61 (wild-type *TRP1*), KKT369 (wild-type *trp1*Δ), KKT402 (*tat2*Δ), KKT403 (*dnf1*Δ), KKT404 (*dnf2*Δ), KKT405 (*dnf1*Δ *dnf2*Δ), KKT406 (*drs2*Δ), KKT372 (*lem3*Δ), KKT433 (*cdc50*Δ), KKT434 (*fpk1*Δ *fpk2*Δ), and KKT407 (*cho1*Δ). These were *trp1*Δ background strains except for KKT61. *C*, Suppression of tryptophan requirement of flippase and flippase-related mutants by over-production of Tat2p. Cell growth was examined as in *A*. Strains were KKT372 (*lem3*Δ), KKT434 (*fpk1*Δ *fpk2*Δ), and KKT407 (*cho1*Δ) harboring YEplac195 (vector) or pKT1747 (YEp-TAT2). KKT369 was used as a WT control. *D*, The *lem3*Δ *tat1*Δ *trp1*Δ mutant exhibits severe tryptophan requirement. Cells were spotted as in *A*, followed by incubation at 25°C for 1.5 days. Strains were KKT369 (wild-type *trp1*Δ), KKT372 (*lem3*Δ), KKT436 (*tat1*Δ), KKT437 (*lem3*Δ *tat1*Δ), KKT402 (*tat2*Δ), and KKT438 (*lem3*Δ *tat2*Δ). These were also *trp1*Δ background strains.

FIGURE 2. **Tagged versions of Tat2p are abnormally regulated or are not fully functional.** Ten-fold serial dilutions of cell suspension were prepared as described in Fig. 1*A*, and spotted on YPDAW and YPDA plates, followed by incubation at 30°C for 22 hours. *A*, Strains were KKT372 (*lem3*Δ), KKT459 (*TAT2-GFP lem3*Δ), KKT460 (*TAT2-GST lem3*Δ), and KKT461 (*TAT2-13myc lem3*Δ). *B*, Strains were KKT369 (wild-type *trp1*Δ) and KKT462 (*TAT2-3HA*). *C*, Strains were KKT381 (wild-type *trp1*Δ/*trp1*Δ) and KKT418 (*tat2*Δ/*tat2*Δ *trp1*Δ/*trp1*Δ) harboring YCplac33 (vector), pKT1765 (YCp-TAT2), pKT1763 (YCp-2HA-TAT2), pKT1742 (YCp-3HA-TAT2), pKT2045 (YCp-P_{ACT1}-3myc-TAT2), and pKT2046 (YCp-P_{ACT1}-GFP-TAT2). These were *trp1*Δ background strains.

FIGURE 3. **Mislocalization of Tat2p in the *lem3*Δ mutant.** *A*, Detection of Tat2p by anti-Tat2p antibodies. Protein extracts from bulk membrane-fraction after centrifugation at 100,000 × g were subjected to immunoblotting with antibodies against the NH_2-terminal cytoplasmic region of Tat2p. α-N1 and -N2 indicate anti-Tat2pN1 and -Tat2pN2 antibodies, respectively. Strains were KKT369 (wild-type *trp1*Δ) and KKT402 (*tat2*Δ *trp1*Δ). *B*, The effect of extracellular tryptophan concentration on the expression level of Tat2p. Total cell lysates prepared from cells of KKT61 (wild-type *TRP1*) were subjected to immunoblotting with the anti-Tat2pN1 or -Kex2p (a loading control) antibodies. The cells were grown to early log phase in SDA medium containing 200 (200W), 30 (30W), or 0 (-W) μg/ml of tryptophan at 30°C. *C*, The effect of extracellular tryptophan concentration on the subcellular distribution

of Tat2p. Total cell lysates prepared from the KKT61 cells grown as described in *B* were subjected to sucrose gradient fractionation as described in the EXPERIMENTAL PROCEDURES, followed by immunoblotting with antibodies against Tat2p, Pma1p, Kex2p, and Pep12p. PM and IMs indicate the plasma membrane-rich fraction and internal membranes-rich fractions, respectively. Distribution of Pma1p, Kex2p, and Pep12p were not affected by extracellular tryptophan concentration (data not shown). *D*, Mislocalization of Tat2p in the *lem3*Δ mutant. Subcellular distribution of Tat2p was examined by sucrose gradient fractionation as in *C*. Cells were grown in SDA-W medium at 30°C or 18°C. Strains were KKT61 (wild-type *TRP1*), KKT102 (*lem3*Δ), KKT268 (*fpk1*Δ *fpk2*Δ), and KKT439 (*cho1*Δ). For the *cho1*Δ mutant, 1 mM ethanolamine was supplemented to the culture medium. *E*, Mislocalization of Tat2p in the *lem3*Δ *trp1*Δ mutant. Subcellular distribution of Tat2p was examined as in *C*. Cells were grown in YPDA medium at 30°C. Strains were KKT369 (wild-type *trp1*Δ) and KKT372 (*lem3*Δ *trp1*Δ). *F*. Vacuole-dependent degradation of Tat2p in the *lem3*Δ mutant. Total cell lysates prepared from cells grown in SDA-W medium at 18°C were subjected to immunoblotting with the anti-Tat2pN1 or -Kex2p (a loading control) antibodies. Strains were KKT61 (wild-type *TRP1*), KKT102 (*lem3*Δ), KKT452 (*pep4*Δ *prb1*Δ), and KKT455 (*lem3*Δ *pep4*Δ *prb1*Δ). These were *TRP1* background strains.

FIGURE 4. **Tat2p is redelivered to the plasma membrane by inhibition of the vacuolar sorting pathway in the *lem3*Δ mutant.** *A*, Suppression of tryptophan requirement in the *lem3*Δ mutant. Ten-fold serial dilutions of cell suspension were prepared as described in Fig. 1*A* and spotted on YPDAW and YPDA plates, followed by incubation at 30°C for 22 hours. Strains were KKT369 (wild-type), KKT372 (*lem3*Δ), KKT429 (*vps1*Δ), KKT430 (*lem3*Δ *vps1*Δ), KKT419 (*gga1*Δ *gga2*Δ), KKT420 (*lem3*Δ *gga1*Δ *gga2*Δ), KKT421 (*pep12*Δ), KKT422 (*lem3*Δ *pep12*Δ), KKT423 (*vps27*Δ), and KKT424 (*lem3*Δ *vps27*Δ). These were *trp1*Δ background strains. *B*, Restoration of the plasma membrane localization of Tat2p in the *lem3*Δ mutant. The cells of strains in *A* were grown in YPDA at 30°C and the PM-rich fractions were isolated, followed by immunoblotting with anti-Tat2pN1 (upper panel) or -Pma1p (lower panel, a loading control) antibodies as described in Fig. 3*C*. *C*, Co-localization of Dnf1p-GFP and Dnf2p-GFP with Sec7p-mRFP. Cells were grown to early log phase in YPDA at 30°C, followed by fluorescence microscopic observation after fixation in 3.7% formaldehyde. Strains used were KKT444 (*DNF1-GFP SEC7-mRFP*, upper panel) and KKT445 (*DNF2-GFP SEC7-mRFP*, lower panel). Images were merged to compare two signal patterns. Arrowheads indicate co-localization between Dnf1p-GFP or Dnf2p-GFP and Sec7p-mRFP. Bars, 5 μm.

FIGURE 5. **Mislocalization of Tat2p in endocytosis-defective mutants.** *A*, Tryptophan requirement in

endocytosis-defective mutants. Ten-fold serial dilutions of cell suspension were prepared and spotted on YPDAW and YPDA plates as in Fig. 1*A*, followed by incubation at 25°C for 1.5 days. Stains were KKT369 (wild-type *trp1*Δ), KKT440 (*end3*Δ), KKT441 (*vrp1*Δ), and KKT440 and KKT441 containing pKT1747 (YEp-TAT2). These were *trp1*Δ background strains. *B*, Subcellular distribution of Tat2p in endocytosis-defective mutants. The cells of KKT61 (wild-type *TRP1*), KKT290 (*end3*Δ *TRP1*), and KKT144 (*vrp1*Δ *TRP1*) were grown in SDA-W medium at 25°C and the cell lysates were subjected to sucrose gradient fractionation, followed by immunoblotting with anti-Tat2pN1 antibodies. *C*, Accumulation of Dnf1p-GFP and Dnf2p-GFP at the plasma membrane in endocytosis-defective mutants. The cells of wild-type and *end3*Δ strains expressing either Dnf1p-GFP or Dnf2p-GFP were grown to early log phase in YPDA at 25°C, followed by fluorescence microscopic observation. Strains were KKT33 (*DNF1-GFP*), KKT334 (*DNF2-GFP*), KKT442 (*end3*Δ *DNF1-GFP*), and KKT443 (*end3*Δ *DNF2-GFP*). Bars, 5 μm. *D*, Tryptophan requirement in the *ypt6*Δ mutant. Cell growth was examined as in Fig. 1*A* at 30°C for 22 h. Strains were KKT369 (wild-type *trp1*Δ), KKT372 (*lem3*Δ), KKT453 (*ypt6*Δ), and KKT454 (*lem3*Δ *ypt6*Δ). These were *trp1*Δ background strains.

FIGURE 6. **Inhibition of ubiquitination restores the plasma membrane localization of Tat2p in the *lem3*Δ mutant.** *A*, Suppression of tryptophan requirement in the *lem3*Δ mutant by mutations in ubiquitination machinery. Ten-fold serial dilutions of cell suspension were prepared and spotted on YPDAW and YPDA plates as in Fig. 1*A*, followed by incubation at 30°C for 22 hours. Strains were KKT369 (wild-type *trp1*Δ), KKT372 (*lem3*Δ), KKT427 ($TAT2^{3K>R}$), KKT428 (*lem3*Δ $TAT2^{3K>R}$), KKT425 (*bul1*Δ *bul2*Δ), KKT426 (*lem3*Δ *bul1*Δ *bul2*Δ), KKT446 (*rsp5-1*), and KKT447 (*lem3*Δ *rsp5-1*). These were *trp1*Δ background strains. *B*, Restoration of the plasma membrane localization of Tat2p in the *lem3*Δ mutant. The cells of strains in *A* were grown in YPDA at 30°C and the PM-rich fractions were isolated by sucrose gradient fractionation, followed by immunoblotting with anti-Tat2pN2 (upper panel) or -Pma1p (lower panel, a loading control) antibodies as described in Fig. 3*C*. *C*, Suppression of tryptophan requirement in *end* mutants, by mutations in ubiquitination machinery. Ten-fold serial dilutions of cell suspension were prepared and spotted on YPDAW and YPDA plates as in Fig. 1*A*, followed by incubation at 25°C for 1.5 days. Strains were KKT369 (wild-type *trp1*Δ), KKT440 (*end3*Δ), KKT448 (*end3*Δ $TAT2^{3K>R}$), KKT449 (*end3*Δ *bul1*Δ), KKT441 (*vrp1*Δ), KKT450 (*vrp1*Δ $TAT2^{3K>R}$), and KKT451 (*vrp1*Δ *bul1*Δ). These were *trp1*Δ background strains.

FIGURE 7. **Tryptophan uptake activity of Tat2p in the *lem3*Δ mutant.** *A*, Tryptophan uptake in the *lem3*Δ and *tat2*Δ mutants. Tryptophan import activity was assayed with L-[5-^{3}H]tryptophan as described

in the EXPERIMENTAL PROCEDURES. The data represent means ± SD of three independent experiments. Strains were KKT61 (wild-type *TRP1*), KKT102 (*lem3*Δ), KKT458 (*tat2*Δ), and KKT465 (*lem3*Δ *tat2*Δ). These were *TRP1* background strains. *B*, Tryptophan uptake activity of Tat2p was not affected by the *lem3*Δ mutation. *Upper panel*, Tat2p content in the PM-rich fraction. PM-rich fractions were isolated by sucrose gradient fractionation from KKT61 (wild-type *TRP1*) harboring YCplac33 (vector) and KKT102 (*lem3*Δ *TRP1*) harboring pKT1765 (YCp-TAT2), followed by immunoblotting with anti-Tat2pN2 or -Pma1p (a loading control) antibodies. The plasma membrane Tat2p level in the *lem3*Δ mutant was 129 ± 15% of the wild type. *Lower panel*, Tryptophan uptake activity of Tat2p. Tryptophan import activity (10^4 dpm/OD_{600}), which was assayed as described in *A*, was corrected for the difference of Tat2p content in the PM-rich fraction.

FIGURE 8. **Mutational analysis of basic residues in the NH_2-terminal region of Tat2p for interaction with liposomes and *in vivo* functions.** *A*, The NH_2-terminal region of Tat2p preferentially binds to PS-containing liposomes. Liposome flotation experiments were performed with GST-Tat2p(residues 1-85) (GST-Tat2pNT) as described in the EXPERIMENTAL PROCEDURES. T, M, and B indicate top, middle, and bottom fractions, respectively. Percent Tat2p in the top fraction is shown (mean ± SD of three independent experiments). The liposome composition was 100 mol% DOPC (PC), 80% DOPC and 20% DOPS (20% PS), 80% DOPC and 20% DOPE (20% PE), 80% DOPC and 20% PA (20% PA), or 80% DOPC and 20% PI (20% PI). Arrowheads indicate GST-Tat2pNT. *B*, Alanine substitution mutations in the NH_2-terminal region of Tat2p. Partial amino acid sequence of the NH_2-terminal region (residues 1-85) and three alanine substitution mutants are shown. Asterisks indicate ubiquitin acceptor lysines. *C*, Interaction of Tat2pNT mutant proteins with PS liposomes. Binding of GST-fused mutant Tat2pNT to PS liposomes (80% DOPC and 20% DOPS) was examined by liposome flotation experiments as in *A*. *D*, Tryptophan-dependent growth phenotypes of the *tat2* mutants. Ten-fold serial dilutions of cell suspension were prepared and spotted on YPDAW and YPDA plates as in Fig. 1*A*, followed by incubation at 30°C for 22 hours. Strains were KKT381 (wild-type *trp1*Δ/*trp1*Δ) and KKT418 (*tat2*Δ/*tat2*Δ) and KKT456 (*lem3*Δ/*lem3*Δ *tat2*Δ/*tat2*Δ) harboring YCplac33 (vector), pKT1765 (*TAT2*), pKT2019 ($TAT2^{5K>A}$), pKT2020 ($TAT2^{2R>A}$), or pKT2021 ($tat2^{2K2R>A}$). These were *trp1*Δ background strains. *E*, Subcellular distribution of mutant Tat2 proteins. Cells were grown to early log phase in SDA-UW medium at 30°C, and the cell lysates were subjected to sucrose gradient fractionation, followed by immunoblotting with anti-Tat2pN1 (α-N1) and -Tat2pN2 (α-N2) antibodies. $Tat2p^{5K>A}$ exhibited mobility shifts possibly because of posttranslational modifications or structural alteration by substitutions. An arrowhead indicates the original Tat2p position. Strains were KKT458 (*tat2*Δ *TRP1*) harboring pKT1765 (Tat2p), pKT2021

(Tat2p$^{2K2R>A}$), pKT2019 (Tat2p$^{5K>A}$), or pKT2020 (Tat2p$^{2R>A}$). *F*, Suppression of tryptophan-dependent growth in the *tat2*$^{2K2R>A}$ mutant by *bul1*Δ *bul2*Δ mutations. Cell growth was examined as described in *D*. Strains were KKT369 (wild-type *trp1*Δ), and KKT457 (*bul1*Δ *bul2*Δ *tat2*Δ *trp1*Δ) harboring YCplac33 (vector), pKT1765 (*TAT2*), or pKT2021 (*tat2*$^{2K2R>A}$).

TABLE 1. **Yeast strains used in this study**

Strain[a]	Relevant genotype	Derivation/source
BY4743	*MATa/α LYS2/lys2Δ0 ura3Δ0/ura3Δ0 his3Δ1/his3Δ1 TRP1/TRP1 leu2Δ0/leu2Δ0 met15Δ0/MET15*	(29)
KKT33	*MATa lys2Δ0 ura3Δ0 his3Δ1 TRP1 leu2Δ0 met15Δ0 DNF1-GFP::HIS3MX6*	(15)
KKT61	*MATa LYS2 ura3Δ0 his3Δ1 TRP1 leu2Δ0 MET15*	(15)
KKT102	*MATa LYS2 ura3Δ0 his3Δ1 TRP1 leu2Δ0 MET15 lem3Δ::KanMX6*	(15)
KKT144	*MATα lys2Δ0 ura3Δ0 his3Δ1 TRP1 leu2Δ0 met15Δ0 vrp1Δ::LEU2*	This study
KKT268	*MATa LYS2 ura3Δ0 his3Δ1 TRP1 leu2Δ0 MET15 fpk1Δ::HphMX4 fpk2Δ::KanMX6*	(15)
KKT290	*MATα lys2Δ0 ura3Δ0 his3Δ1 TRP1 leu2Δ0 met15Δ0 end3Δ::HphMX4*	This study
KKT334	*MATa LYS2 ura3Δ0 his3Δ1 TRP1 leu2Δ0 MET15 DNF2-GFP::HIS3MX6*	(15)
KKT369	*MATa LYS2 ura3Δ0 his3Δ1 trp1Δ-63 leu2Δ0 MET15*	This study
KKT372	*MATa LYS2 ura3Δ0 his3Δ1 trp1Δ-63 leu2Δ0 MET15 lem3Δ::KanMX6*	This study
KKT381	*MATa/α LYS2/LYS2 ura3Δ0/ura3Δ0 his3Δ1/his3Δ1 trp1Δ-63/trp1Δ-63 leu2Δ0/leu2Δ0 MET15/MET15*	This study
KKT402	*MATa LYS2 ura3Δ0 his3Δ1 trp1Δ-63 leu2Δ0 MET15 tat2Δ::KanMX4*	This study
KKT403	*MATα LYS2 ura3Δ0 his3Δ1 trp1Δ-63 leu2Δ0 MET15 dnf1Δ::HphMX4*	This study
KKT404	*MATa LYS2 ura3Δ0 his3Δ1 trp1Δ-63 leu2Δ0 MET15 dnf2Δ::KanMX4*	This study
KKT405	*MATa LYS2 ura3Δ0 his3Δ1 trp1Δ-63 leu2Δ0 MET15 dnf1Δ::HphMX4 dnf2Δ::KanMX4*	This study
KKT406	*MATα lys2Δ0 ura3Δ0 his3Δ1 trp1Δ-63 leu2Δ0 MET15 drs2Δ::KanMX4*	This study
KKT407	*MATα lys2Δ0 ura3Δ0 his3Δ1 trp1Δ-63 leu2Δ0 MET15 cho1Δ::HIS3MX6*	This study
KKT418	*MATa/α LYS2/LYS2 ura3Δ0/ura3Δ0 his3Δ1/his3Δ1 trp1Δ-63/trp1Δ-63 leu2Δ0/leu2Δ0 MET15/MET15 tat2Δ::KanMX4/tat2Δ::KanMX4*	This study
KKT419	*MATa LYS2 ura3Δ0 his3Δ1 trp1Δ-63 leu2Δ0 met15Δ0 gga1Δ:: HIS3MX6 gga2Δ::KanMX4*	This study
KKT420	*MATα LYS2 ura3Δ0 his3Δ1 trp1Δ-63 leu2Δ0 met15Δ0 lem3Δ::KanMX6 gga1Δ::HIS3MX6 gga2Δ::KanMX4*	This study
KKT421	*MATa LYS2 ura3Δ0 his3Δ1 trp1Δ-63 leu2Δ0 MET15 pep12Δ::KanMX4*	This study
KKT422	*MATα LYS2 ura3Δ0 his3Δ1 trp1Δ-63 leu2Δ0 MET15 lem3Δ::HIS3MX6 pep12Δ::KanMX4*	This study
KKT423	*MATa LYS2 ura3Δ0 his3Δ1 trp1Δ-63 leu2Δ0 MET15 vps27Δ::HIS3*	This study
KKT424	*MATa LYS2 ura3Δ0 his3Δ1 trp1Δ-63 leu2Δ0 MET15 lem3Δ::KanMX6 vps27Δ::HIS3*	This study
KKT425	*MATa LYS2 ura3Δ0 his3Δ1 trp1Δ-63 leu2Δ0 MET15 bul1Δ::HIS3MX6 bul2Δ::KanMX6*	This study
KKT426	*MATa LYS2 ura3Δ0 his3Δ1 trp1Δ-63 leu2Δ0 MET15 lem3Δ::KanMX6 bul1Δ::HIS3MX6 bul2Δ::KanMX6*	This study
KKT427	*MATa LYS2 ura3Δ0 his3Δ1 trp1Δ-63 leu2Δ0 MET15 TAT2*$^{3K>R}$	This study
KKT428	*MATa LYS2 ura3Δ0 his3Δ1 trp1Δ-63 leu2Δ0 MET15 lem3Δ::HIS3MX6 TAT2*$^{3K>R}$	This study

KKT429	*MATa LYS2 ura3Δ0 his3Δ1 trp1Δ-63 leu2Δ0 met15Δ0 vps1Δ::KanMX4*	This study
KKT430	*MATα lys2Δ0 ura3Δ0 his3Δ1 trp1Δ-63 leu2Δ0 MET15 lem3Δ::HIS3MX6 vps1Δ::KanMX4*	This study
KKT433	*MATa LYS2 ura3Δ0 his3Δ1 trp1Δ-63 leu2Δ0 MET15 cdc50Δ::HphMX4*	This study
KKT434	*MATa LYS2 ura3Δ0 his3Δ1 trp1Δ-63 leu2Δ0 MET15 fpk1Δ::HphMX4 fpk2Δ::KanMX6*	This study
KKT435	*MATa LYS2 ura3Δ0 his3Δ1 trp1Δ-63 leu2Δ0 met15Δ0 psd1Δ::KanMX4 psd2Δ::HIS3MX6*	This study
KKT436	*MATa LYS2 ura3Δ0 his3Δ1 trp1Δ-63 leu2Δ0 MET15 tat1Δ::HIS3MX6*	This study
KKT437	*MATa LYS2 ura3Δ0 his3Δ1 trp1Δ-63 leu2Δ0 MET15 lem3Δ::KanMX6 tat1Δ::HIS3MX6*	This study
KKT438	*MATa LYS2 ura3Δ0 his3Δ1 trp1Δ-63 leu2Δ0 MET15 lem3Δ::HIS3MX6 tat2Δ::KanMX4*	This study
KKT439	*MATa lys2Δ0 ura3Δ0 his3Δ1 TRP1 leu2Δ0 met15Δ0 cho1Δ::KanMX6*	This study
KKT440	*MATα lys2Δ0 ura3Δ0 his3Δ1 trp1Δ-63 leu2Δ0 MET15 end3Δ::HphMX4*	This study
KKT441	*MATα lys2Δ0 ura3Δ0 his3Δ1 trp1Δ-63 leu2Δ0 met15Δ0 vrp1Δ::LEU2*	This study
KKT442	*MATa lys2Δ0 ura3Δ0 his3Δ1 TRP1 leu2Δ0 met15Δ0 end3Δ::HphMX4 DNF1-GFP::HIS3MX6*	This study
KKT443	*MATa lys2Δ0 ura3Δ0 his3Δ1 TRP1 leu2Δ0 met15Δ0 end3Δ::HphMX4 DNF2-GFP::HIS3MX6*	This study
KKT444	*MATa lys2Δ0 ura3Δ0 his3Δ1 TRP1 leu2Δ0 met15Δ0 DNF1-GFP::HIS3MX6 SEC7-mRFP1::HIS3MX6*	This study
KKT445	*MATa LYS2 ura3Δ0 his3Δ1 TRP1 leu2Δ0 met15Δ0 DNF2-GFP::HIS3MX6 SEC7-mRFP1::HIS3MX6*	This study
KKT446	*MATα LYS2 ura3Δ0 his3Δ1 trp1Δ-63 leu2Δ0 MET15 rsp5-1*	This study
KKT447	*MATα LYS2 ura3Δ0 his3Δ1 trp1Δ-63 leu2Δ0 MET15 lem3Δ::KanMX6 rsp5-1*	This study
KKT448	*MATa LYS2 ura3Δ0 his3Δ1 trp1Δ-63 leu2Δ0 MET15 end3Δ::HphMX4 TAT2$^{3K>R}$*	This study
KKT449	*MATa lys2Δ0 ura3Δ0 his3Δ1 trp1Δ-63 leu2Δ0 met15Δ0 end3Δ::HphMX4 bul1Δ::HIS3MX6*	This study
KKT450	*MATa LYS2 ura3Δ0 his3Δ1 trp1Δ-63 leu2Δ0 MET15 vrp1Δ::LEU2 TAT2$^{3K>R}$*	This study
KKT451	*MATα LYS2 ura3Δ0 his3Δ1 trp1Δ-63 leu2Δ0 met15Δ0 vrp1Δ::LEU2 bul1Δ::HIS3MX6*	This study
KKT452	*MATa LYS2 ura3Δ0 his3Δ1 TRP1 leu2Δ0 MET15 pep4Δ::KanMX4 prb1Δ::NatMX4*	This study
KKT453	*MATa lys2Δ0 ura3Δ0 his3Δ1 trp1Δ-63 leu2Δ0 met15Δ0 ypt6Δ::KanMX4*	This study
KKT454	*MATa lys2Δ0 ura3Δ0 his3Δ1 trp1Δ-63 leu2Δ0 met15Δ0 lem3Δ::HIS3MX6 ypt6Δ::KanMX4*	This study
KKT455	*MATa LYS2 ura3Δ0 his3Δ1 TRP1 leu2Δ0 MET15 lem3Δ::HIS3MX6 pep4Δ::KanMX4 prb1Δ::NatMX4*	This study
KKT456	*MATa/α LYS2/LYS2 ura3Δ0/ura3Δ0 his3Δ1/his3Δ1 trp1Δ-63/trp1Δ-63 leu2Δ0/leu2Δ0 MET15/MET15 lem3Δ::HIS3MX6/lem3Δ::HIS3MX6 tat2Δ::KanMX4/tat2Δ::KanMX4*	This study
KKT457	*MATα LYS2 ura3Δ0 his3Δ1 trp1Δ-63 leu2Δ0 MET15 tat2Δ::KanMX4 bul1Δ::HIS3MX6 bul2Δ::KanMX6*	This study
KKT458	*MATa LYS2 ura3Δ0 his3Δ1 TRP1 leu2Δ0 met15Δ0 tat2Δ::KanMX4*	This study
KKT459	*MATa LYS2 ura3Δ0 his3Δ1 trp1Δ-63 leu2Δ0 MET15 TAT2-GFP::HIS3MX6 lem3Δ::KanMX6*	This study
KKT460	*MATa LYS2 ura3Δ0 his3Δ1 trp1Δ-63 leu2Δ0 MET15 TAT2-GST::HIS3MX6 lem3Δ::KanMX6*	This study
KKT461	*MATa LYS2 ura3Δ0 his3Δ1 trp1Δ-63 leu2Δ0 MET15 TAT2-13myc::HIS3MX6 lem3Δ::KanMX6*	This study

KKT462	*MAT*a *LYS2 ura3Δ0 his3Δ1 trp1Δ-63 leu2Δ0 MET15 TAT2-3HA::URA3*	This study
KKT465	*MAT*a *LYS2 ura3Δ0 his3Δ1 TRP1 leu2Δ0 MET15 lem3Δ::HIS3MX6 tat2Δ::KanMX4*	This study

[a] KKT strains are isogenic derivatives of BY4743.

TABLE 2. **Plasmids used in this study**

Plasmid	Characteristics	Derivation/source
YCplac33	*URA3 CEN4*	(76)
YEplac195	*URA3 2μm*	(76)
pKO10	P_{GAL1}*-HA URA3 2μm*	(77)
pGEX	*GST* Amp^R	GE Healthcare
pKU51 [YIplac211-TAT2-3HA]	*TAT2-3HA URA3* Amp^R	(20)
pKU65 [pUC18-vps27Δ]	*vps27Δ::HIS3* Amp^R	(20)
pKT1742 [YCplac33-3HA-TAT2]	*3HA-TAT2 URA3 CEN4*	(78)
pKT1747 [YEplac195-TAT2]	*TAT2 URA3 2μm*	(79)
pKT1763 [YCplac33-2HA-TAT2]	*2HA-TAT2 URA3 CEN4*	(79)
pKT1765 [YCplac33-TAT2]	*TAT2 URA3 CEN4*	This study
pKT1855 [pGEX-GST-TAT2NT]	*GST-TAT2(residues 1-85)* Amp^R	This study
pKT2008 [pBSII-TAT2$^{3K>R}$]	*TAT2*$^{3K>R}$ Amp^R	This study
pKT2019 [YCplac33-TAT2$^{5K>A}$]	*TAT2*$^{5K>A}$ *URA3 CEN4*	This study
pKT2020 [YCplac33-TAT2$^{2R>A}$]	*TAT2*$^{2R>A}$ *URA3 CEN4*	This study
pKT2021 [YCplac33-tat2$^{2K2R>A}$]	*tat2*$^{2K2R>A}$ *URA3 CEN4*	This study
pKT2026 [pKO10-GST-TAT2NT]	P_{GAL1}*-HA-GST-TAT2(residues 1-85) URA3 2μm*	This study
pKT2027 [pKO10-GST-TAT2NT$^{5K>A}$]	P_{GAL1}*-HA-GST-TAT2*$^{5K>A}$*(residues 1-85) URA3 2μm*	This study
pKT2028 [pKO10-GST-TAT2NT$^{2R>A}$]	P_{GAL1}*-HA-GST-TAT2*$^{2R>A}$*(residues 1-85) URA3 2μm*	This study
pKT2029 [pKO10-GST-TAT2NT$^{2K2R>A}$]	P_{GAL1}*-HA-GST-TAT2*$^{2K2R>A}$*(residues 1-85) URA3 2μm*	This study
pKT2045 [pRS316-P_{ACT1}-3myc-TAT2]	P_{ACT1}*-3myc-TAT2 URA3 CEN6*	This study
pKT2046 [pRS316-P_{ACT1}-GFP-TAT2]	P_{ACT1}*-GFP-TAT2 URA3 CEN6*	This study

Figure 1.

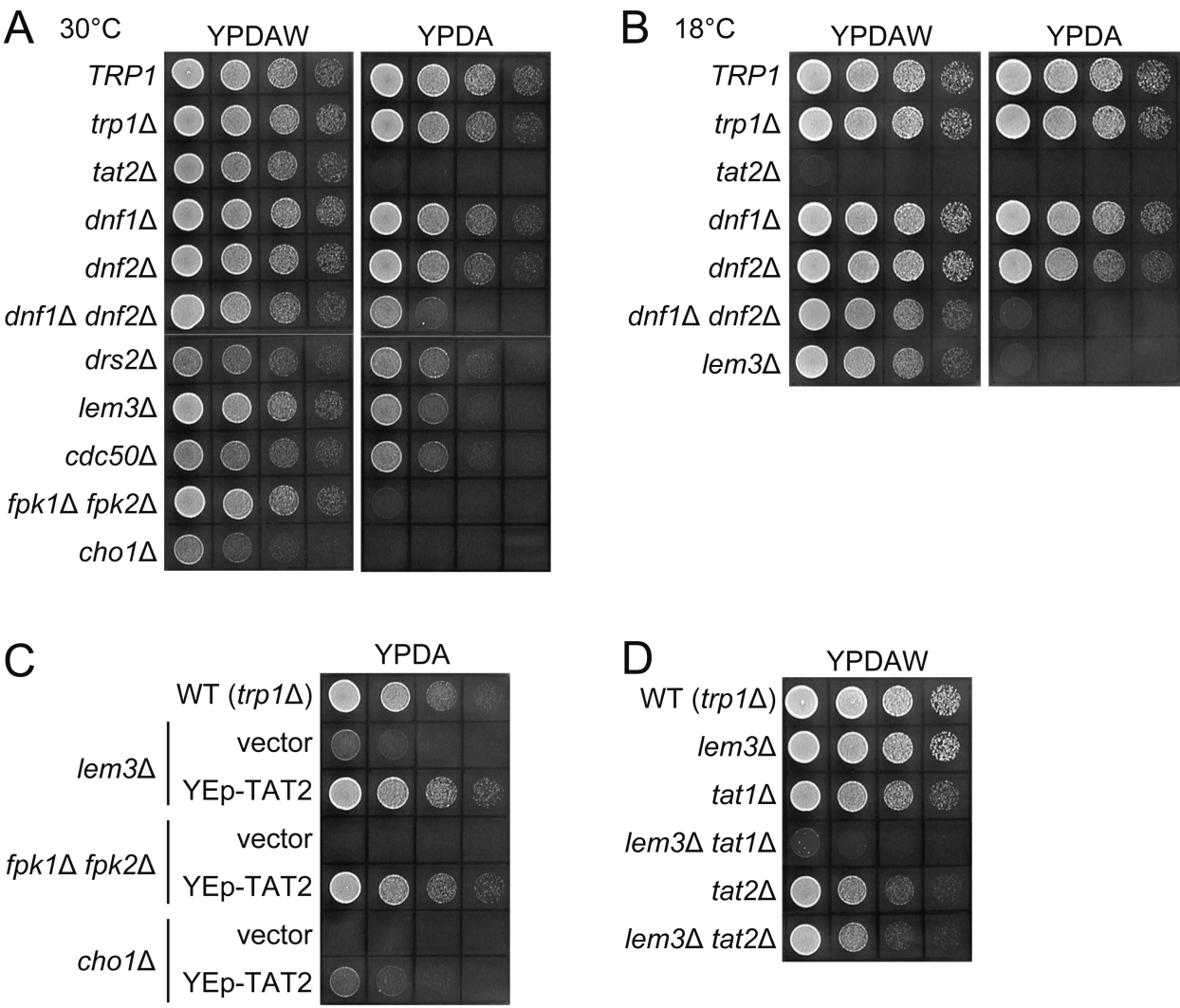
A
30°C
YPDAW
YPDA
TRP1
trp1Δ
tat2Δ
dnf1Δ
dnf2Δ
dnf1Δ dnf2Δ
drs2Δ
lem3Δ
cdc50Δ
fpk1Δ fpk2Δ
cho1Δ
B
18°C
YPDAW
YPDA
TRP1
trp1Δ
tat2Δ
dnf1Δ
dnf2Δ
dnf1Δ dnf2Δ
lem3Δ
C
YPDA
WT (trp1Δ)
lem3Δ
vector
YEp-TAT2
fpk1Δ fpk2Δ
vector
YEp-TAT2
cho1Δ
vector
YEp-TAT2
D
YPDAW
WT (trp1Δ)
lem3Δ
tat1Δ
lem3Δ tat1Δ
tat2Δ
lem3Δ tat2Δ

Figure 2.

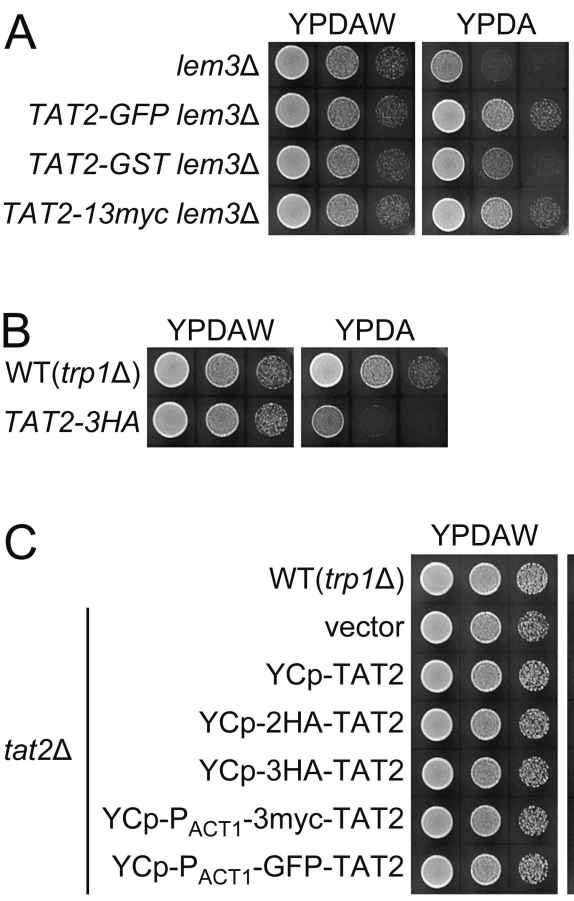
A
YPDAW
YPDA
lem3Δ
TAT2-GFP lem3Δ
TAT2-GST lem3Δ
TAT2-13myc lem3Δ
B
YPDAW
YPDA
WT(trp1Δ)
TAT2-3HA
C
YPDAW
YPDA
WT(trp1Δ)
vector
YCp-TAT2
YCp-2HA-TAT2
YCp-3HA-TAT2
YCp-P$_{ACT1}$-3myc-TAT2
YCp-P$_{ACT1}$-GFP-TAT2
tat2Δ

Figure 3.

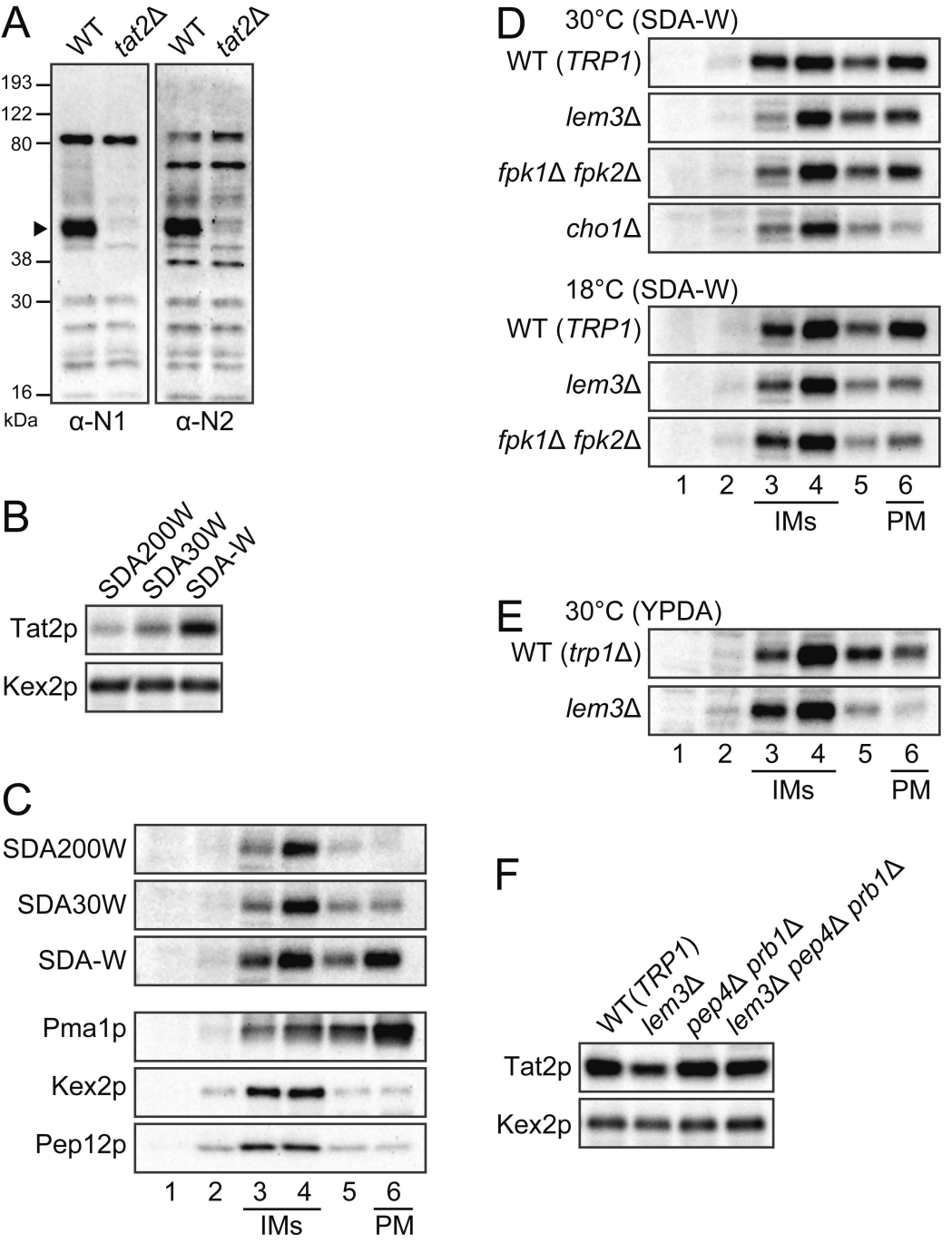
A
WT
tat2Δ
WT
tat2Δ
193
122
80
38
30
16
kDa
α-N1
α-N2
B
SDA200W
SDA30W
SDA-W
Tat2p
Kex2p
C
SDA200W
SDA30W
SDA-W
Pma1p
Kex2p
Pep12p
1 2 3 4 5 6
IMs
PM
D
30°C (SDA-W)
WT (TRP1)
lem3Δ
fpk1Δ fpk2Δ
cho1Δ
18°C (SDA-W)
WT (TRP1)
lem3Δ
fpk1Δ fpk2Δ
1 2 3 4 5 6
IMs
PM
E
30°C (YPDA)
WT (trp1Δ)
lem3Δ
1 2 3 4 5 6
IMs
PM
F
WT(TRP1)
lem3Δ
pep4Δ prb1Δ
lem3Δ pep4Δ prb1Δ
Tat2p
Kex2p

Figure 4.

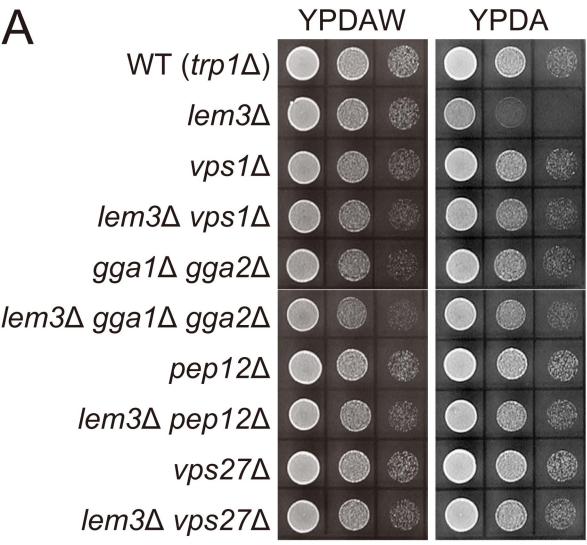
A
YPDAW
YPDA
WT (trp1Δ)
lem3Δ
vps1Δ
lem3Δ vps1Δ
gga1Δ gga2Δ
lem3Δ gga1Δ gga2Δ
pep12Δ
lem3Δ pep12Δ
vps27Δ
lem3Δ vps27Δ

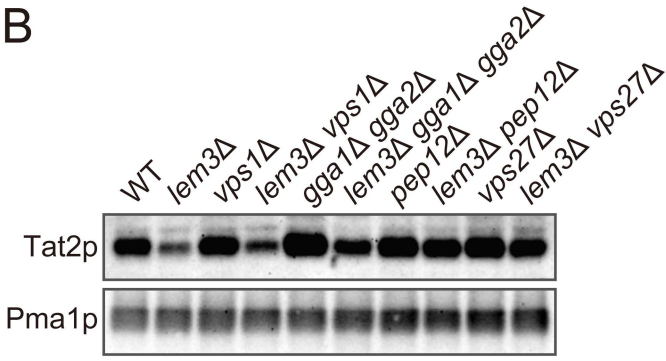
B
WT
lem3Δ
vps1Δ
lem3Δ vps1Δ
gga1Δ gga2Δ
lem3Δ gga1Δ gga2Δ
pep12Δ
lem3Δ pep12Δ
vps27Δ
lem3Δ vps27Δ
Tat2p
Pma1p

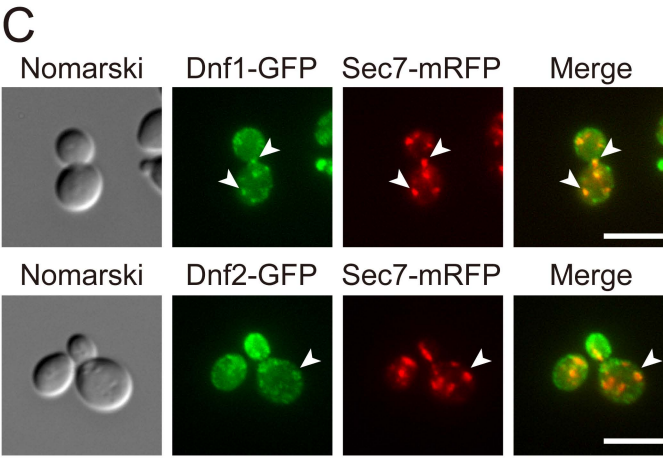
C
Nomarski
Dnf1-GFP
Sec7-mRFP
Merge
Nomarski
Dnf2-GFP
Sec7-mRFP
Merge

Figure 5.

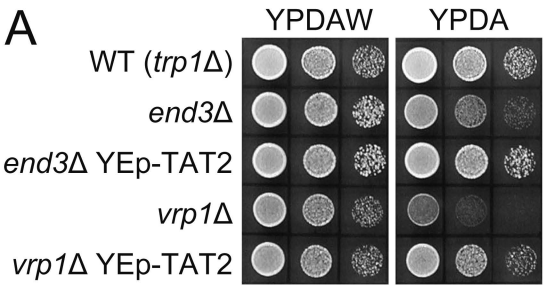
A
YPDAW
YPDA
WT (trp1Δ)
end3Δ
end3Δ YEp-TAT2
vrp1Δ
vrp1Δ YEp-TAT2

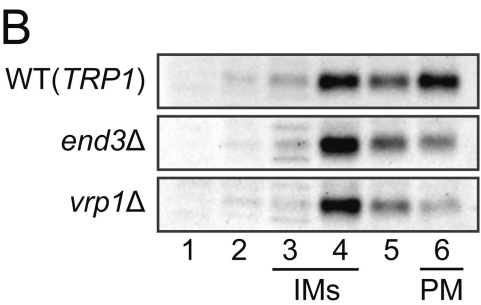
B
WT(TRP1)
end3Δ
vrp1Δ
1 2 3 4 5 6
IMs
PM

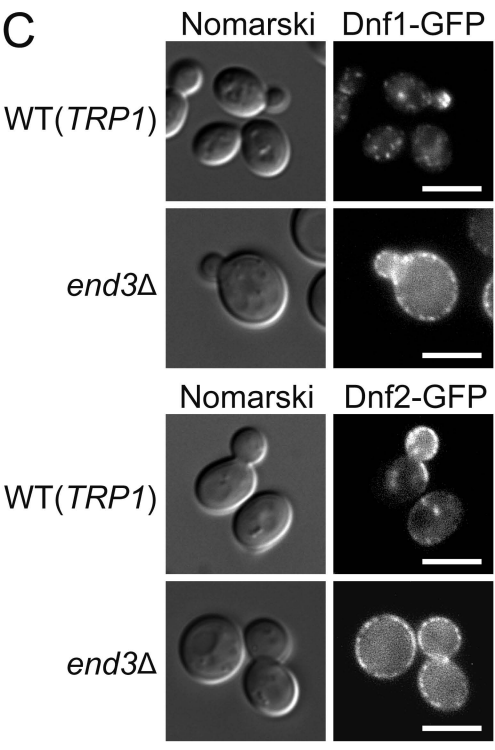
C
Nomarski
Dnf1-GFP
WT(TRP1)
end3Δ
Nomarski
Dnf2-GFP
WT(TRP1)
end3Δ

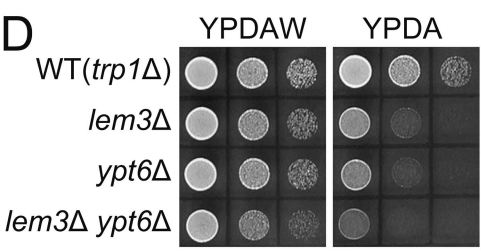
D
YPDAW
YPDA
WT(trp1Δ)
lem3Δ
ypt6Δ
lem3Δ ypt6Δ

Figure 6.

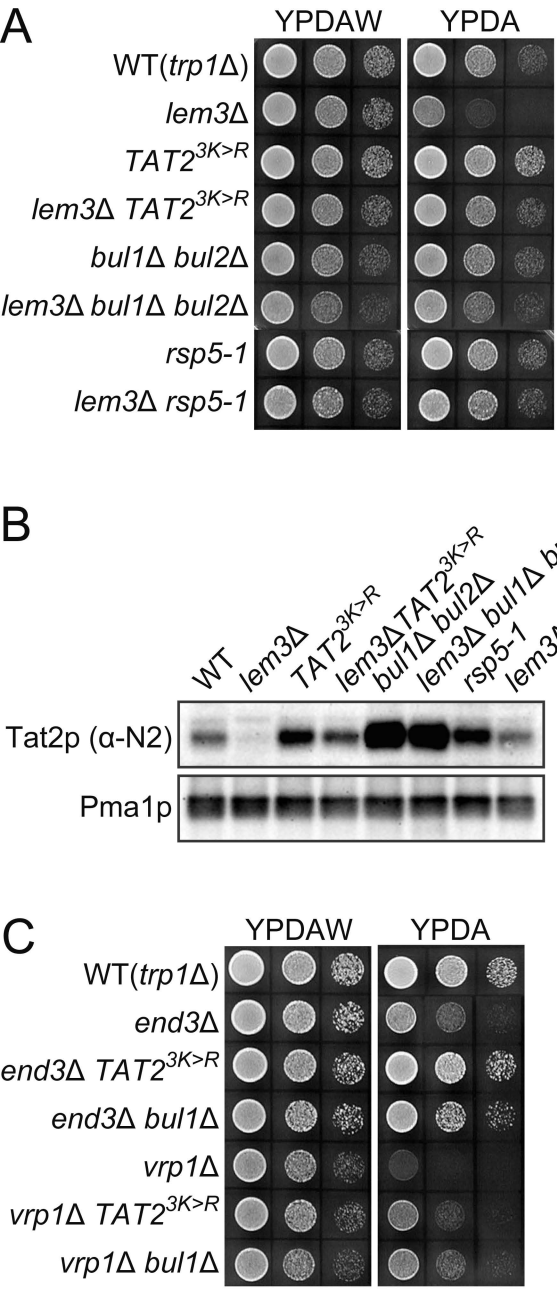
A
YPDAW
YPDA
WT(trp1Δ)
lem3Δ
TAT2^3K>R
lem3Δ TAT2^3K>R
bul1Δ bul2Δ
lem3Δ bul1Δ bul2Δ
rsp5-1
lem3Δ rsp5-1
B
WT
lem3Δ
TAT2^3K>R
lem3ΔTAT2^3K>R
bul1Δ bul2Δ
lem3Δ bul1Δ bul2Δ
rsp5-1
lem3Δ rsp5-1
Tat2p (α-N2)
Pma1p
C
YPDAW
YPDA
WT(trp1Δ)
end3Δ
end3Δ TAT2^3K>R
end3Δ bul1Δ
vrp1Δ
vrp1Δ TAT2^3K>R
vrp1Δ bul1Δ

Figure 7.

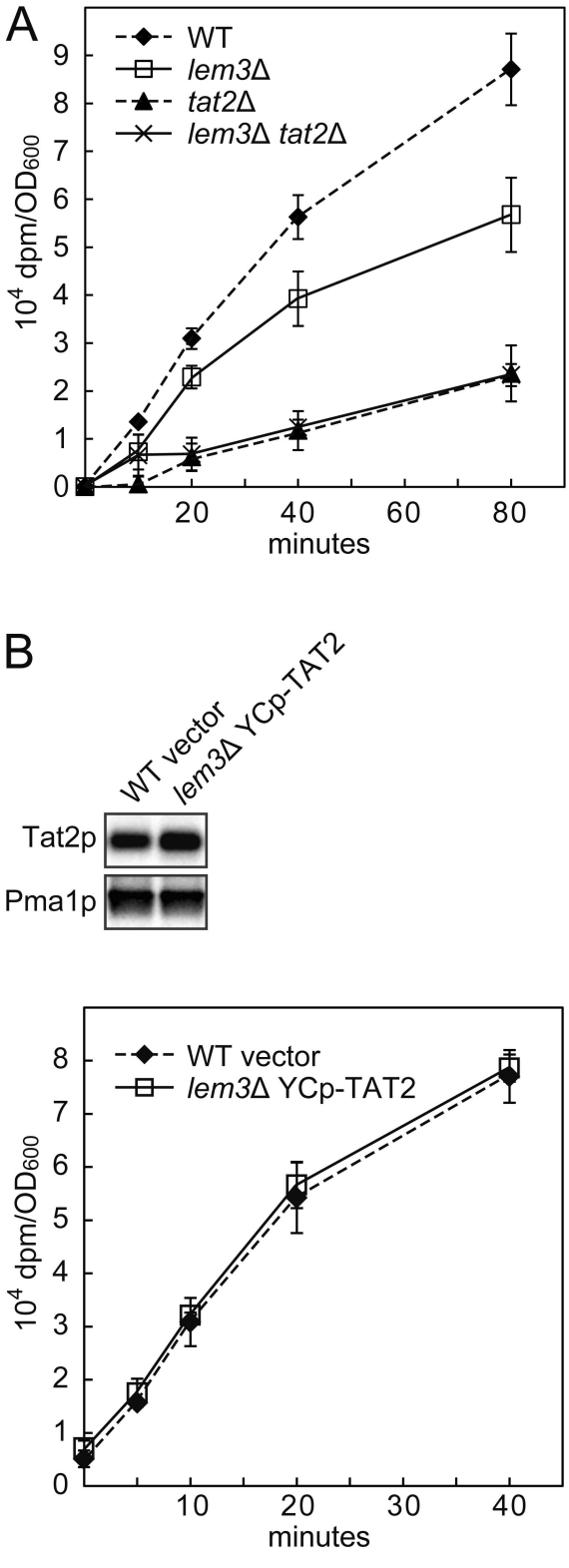
A
WT
lem3Δ
tat2Δ
lem3Δ tat2Δ
10^4 dpm/OD600
minutes
B
WT vector
lem3Δ YCp-TAT2
Tat2p
Pma1p
WT vector
lem3Δ YCp-TAT2
10^4 dpm/OD600
minutes

Figure 8.

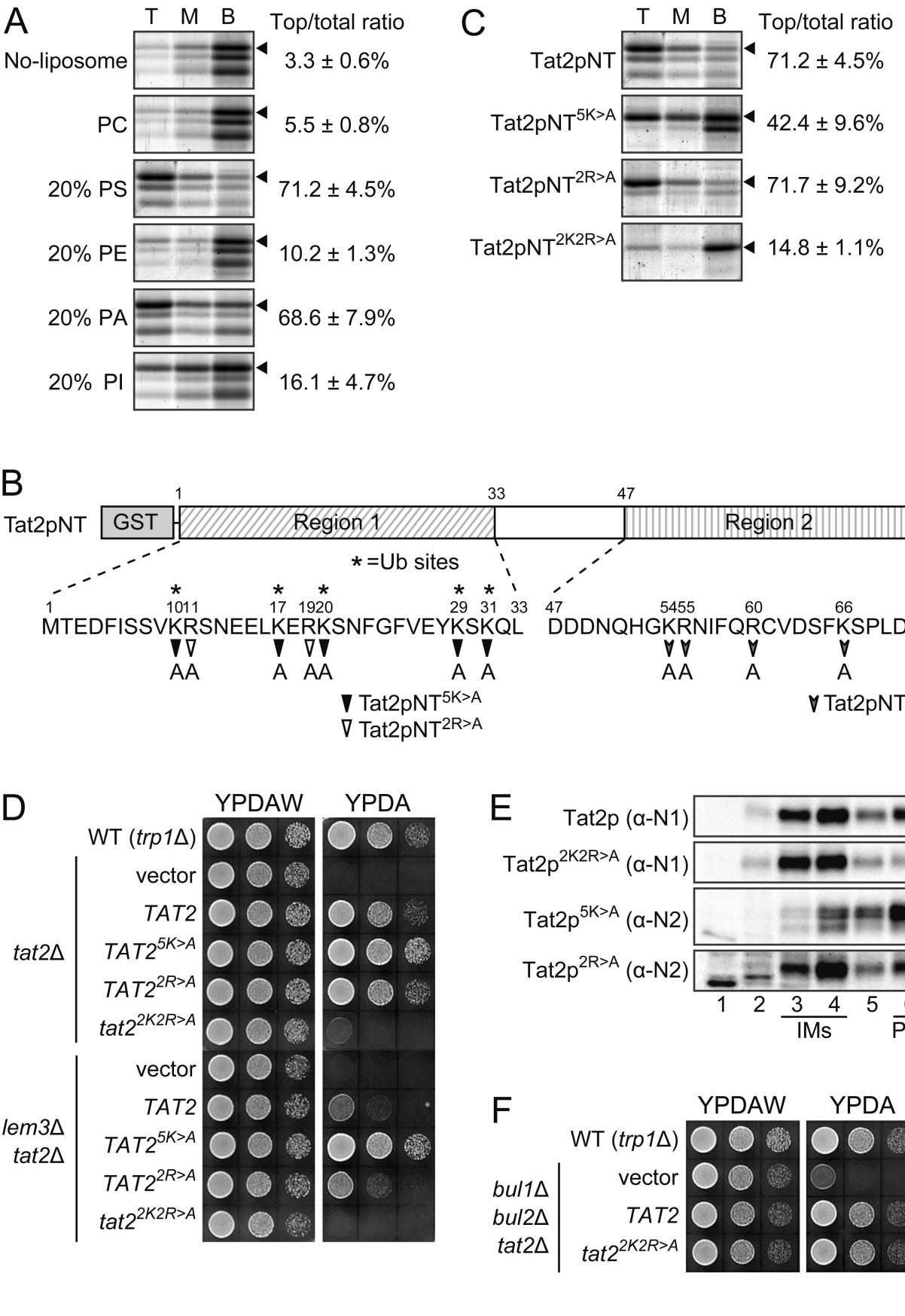
A
T M B
Top/total ratio
No-liposome
3.3 ± 0.6%
PC
5.5 ± 0.8%
20% PS
71.2 ± 4.5%
20% PE
10.2 ± 1.3%
20% PA
68.6 ± 7.9%
20% PI
16.1 ± 4.7%
C
T M B
Top/total ratio
Tat2pNT
71.2 ± 4.5%
Tat2pNT5K>A
42.4 ± 9.6%
Tat2pNT2R>A
71.7 ± 9.2%
Tat2pNT2K2R>A
14.8 ± 1.1%
B
Tat2pNT
GST
Region 1
Region 2
1
33
47
77
85
*=Ub sites
MTEDFISSVKRSNEELKERKSNFGFVEYKSKQL
DDDNQHGKRNIFQRCVDSFKSPLDGSFDTSN
AA
A
AA
A
A
AA
A
A
Tat2pNT5K>A
Tat2pNT2R>A
Tat2pNT2K2R>A
D
YPDAW
YPDA
WT (trp1Δ)
vector
TAT2
TAT25K>A
TAT22R>A
tat22K2R>A
tat2Δ
vector
TAT2
TAT25K>A
TAT22R>A
tat22K2R>A
lem3Δ tat2Δ
E
Tat2p (α-N1)
Tat2p2K2R>A (α-N1)
Tat2p5K>A (α-N2)
Tat2p2R>A (α-N2)
1 2 3 4 5 6
IMs
PM
F
YPDAW
YPDA
WT (trp1Δ)
vector
TAT2
tat22K2R>A
bul1Δ bul2Δ tat2Δ